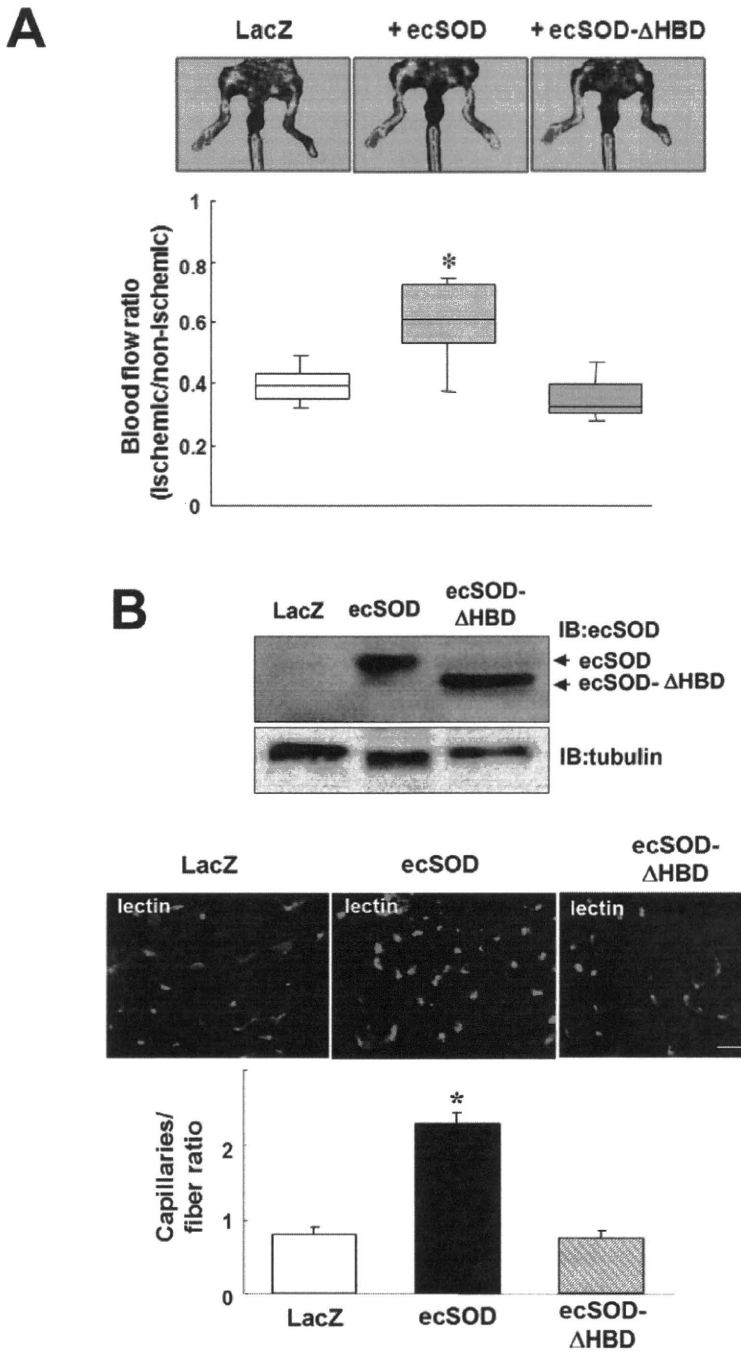

Figure 1. ecSOD gene transfer promotes blood flow recovery and angiogenesis in hindlimb ischemia model. A. C57BL/6J mice were subjected to unilateral hindlimb ischemic surgery and adenoviral injection (Ad.LacZ or Ad.ecSOD or Ad.ecSOD-ΔHBD, 1×10^9 pfu) into adductor muscle was performed at immediately after surgery. Hindlimb blood flow recovery was measured by relative values of laser Doppler perfusion between ischemic and non-ischemic legs at day14 (n = 5–6). **B.** Representative Western blots of adductor muscle lysates obtained after adenoviral injection at day 3 probed by anti-human ecSOD or anti-α-tubulin antibodies. **C.** Mouse adductor muscle tissues were stained by *simplicifolia* lectin to detect capillaries at day7 after ischemia. Capillary density was quantitated as the number of capillaries per muscle fibers. (n = 4). Bar indicates 50 μm. *p<0.05 vs. Ad.LacZ.

doi:10.1371/journal.pone.0010189.g001

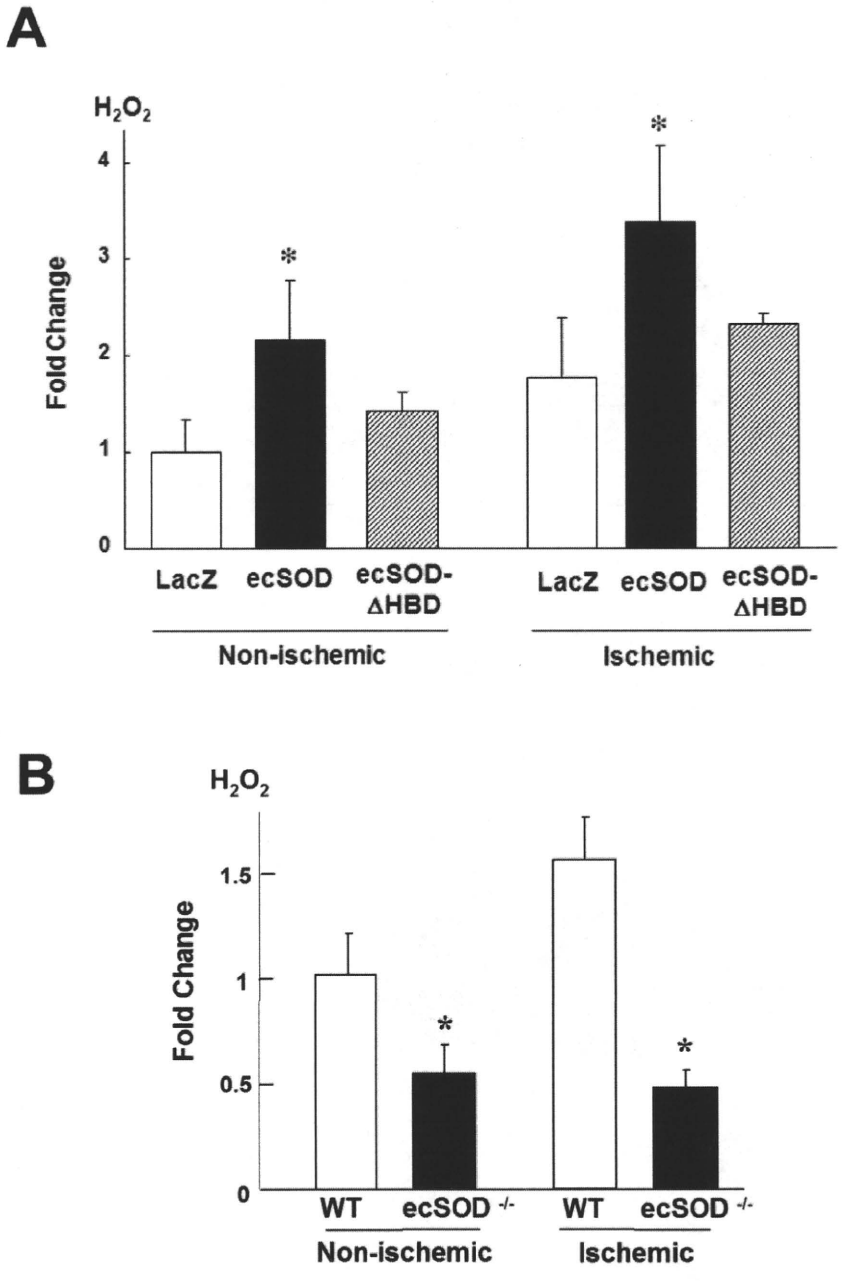

Figure 2. ecSOD increases H_2O_2 levels in non-ischemic and ischemic limbs in hindlimb ischemia model. H_2O_2 levels in non-ischemic and ischemic adductor muscles were measured by Amplex Red from WT mice after adenoviral injection (Ad.LacZ or Ad.ecSOD or Ad.ecSOD-ΔHBD, 1×10^9 pfu) (**A**), or from WT and ecSOD$^{-/-}$ mice (**B**) at day 3 (n = 4–6). The values were normalized by tissue weights and expressed as fold change over LacZ (A) or WT (B) of non-ischemic sites. *p<0.05 vs. LacZ (A) or WT (B).
doi:10.1371/journal.pone.0010189.g002

ecSOD-derived H_2O_2 in VEGF signaling in ECs. Figure 3A shows that infection of HUVECs with Ad.ecSOD significantly enhanced VEGF-induced VEGFR2 autophosphorylation without affecting basal phosphorylation. By contrast, Ad.ecSOD-ΔHBD had no effects on this response under the condition in which both ecSOD and ecSOD-ΔHBD were expressed in cell lysates to similar extent (Fig. 3B). We also verified the protein expression and activity of both ecSOD and ecSOD-ΔHBD in cultured media (Fig. S1). These suggest that newly synthesized ecSOD proteins pass through intracellular secretory pathway to the extracellular space, and that ecSOD bound to ECs surface via HBD, but not ecSOD inside the cells, is required for facilitating VEGF-induced VEGFR2-pY. Consistently, conditioned media of Ad.ecSOD-infected ECs also augmented VEGF-induced receptor phosphorylation (Fig. 3D). Of note, short-term pretreatment with the H_2O_2-detoxifying enzyme catalase that does not enter the cells prevented

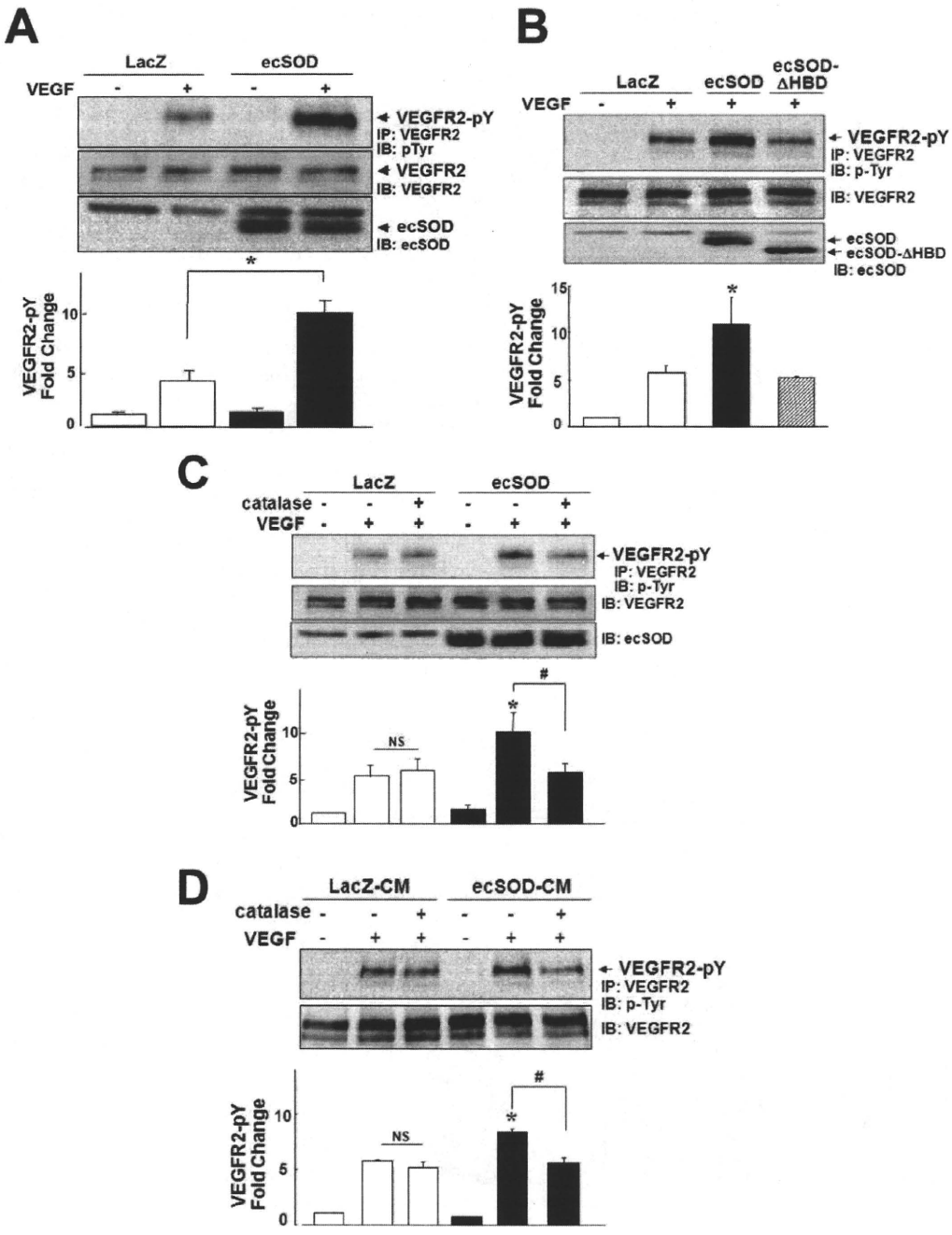

Figure 3. Extracellular H_2O_2 generated by ecSOD enhances VEGF-induced VEGFR2 autophosphorylation, in a HBD-dependent manner, in ECs. A and B. HUVECs were infected with Ad.ecSOD or Ad.LacZ (**A and B**) or Ad.ecSOD-ΔHBD (**B**), and stimulated with VEGF (20 ng/ml) for 5 min. Lysates were immunoprecipitated (IP) with anti-VEGFR2 antibody (Ab), followed by immunoblotted (IB) with anti-phospho-tyrosine (pTyr) Ab to measure VEGFR2-pY. The same lysates were IB with anti-VEGFR2 or ecSOD Abs (n = 3–4). **C.** HUVECs infected with Ad.LacZ or Ad.ecSOD were pretreated with catalase (500 U/ml) for 1 hr to scavenge extracellular H_2O_2, and then stimulated with VEGF (20 ng/ml) for 5 min. Lysates were used for measurement of VEGFR2-pY or total VEGFR2 or ecSOD expression (n = 4). **D.** HUVECs were incubated with conditioned media (CM) obtained from Ad.ecSOD or Ad.LacZ-infected HUVECs for 15 min, and stimulated with VEGF (20 ng/ml) for 5 min. Some cells were pretreated with catalase (500 U/ml) for 15 min to scavenge extracellular H_2O_2 before CM addition. Lysates were used for measurement of VEGFR2-pY or total VEGFR2 (n = 3). Bottom panel shows averaged data; expressed as fold change over basal (means ± S.E.). *$p<0.05$ vs. Ad.LacZ+VEGF. # $p<0.05$.
doi:10.1371/journal.pone.0010189.g003

the effects induced by Ad.ecSOD (Fig. 3C) and conditioned media of Ad.ecSOD-infected ECs (Fig. 3D). By contrast, this exogenous catalase treatment had no effects on VEGF-induced VEGFR2 phosphorylation in LacZ-infected ECs. Either exogenous application of H_2O_2 (<500 μM) which is diffusible (Fig. S2), or NO donor DETA-NO (Fig. S3) had no effects on both basal and VEGF-induced VEGFR2-pY, while higher concentration of H_2O_2 (at 500 μM) only enhanced VEGF-induced this response (Fig. S2). We found that concentration of H_2O_2 in culture medium in Ad.ecSOD-infected ECs was at around 1 μM, as measured by Amplex Red. These suggest that extracellular H_2O_2 derived from ecSOD anchored to ECs surface via HBD is produced locally to promote VEGFR2 phosphorylation.

We next examined whether ecSOD increases H_2O_2 levels in ECs using DCF-DA that detects intracellular peroxides including H_2O_2. Figure 4 shows that overexpression of ecSOD, but not ecSOD-ΔHBD, increased DCF fluorescence compared to Ad.-LacZ-infected cells. Note that some of ecSOD-derived H_2O_2 signals accumulated at plasma membrane, and that short-term treatment of exogenous catalase inhibited ecSOD-induced DCF signal. We confirmed that pretreatment of ECs with polyethylene glycol (PEG)-catalase that enters the cells before loading DCF-DA abolished the fluorescence signals in basal state, as reported previously [38]. Taken together, these suggest that ecSOD binding to ECs via HBD is required to generate extracellular H_2O_2, which enters the cells to regulate VEGF signaling.

ecSOD localized in caveolae/lipid rafts via HBD enhances VEGF-induced VEGFR2 autophoshorylation in these microdomains. Since H_2O_2 is highly diffusible, and some core proteins of HSPGs and VEGFR2 are localized in caveolae/lipid rafts [19,20,28], we next examined whether ecSOD-induced regulation of VEGFR2 may occur in these microdomains. Sucrose gradient fractionation confirmed that VEGFR2 was localized in caveolin-1-enriched, low density lipid rafts fraction 4–6 (Fig. 5A). Intriguingly, ecSOD overexpression increased its localization in both caveolae/lipid rafts and non-caveolae/lipid rafts fractions (Fraction 9–13), while ecSOD-ΔHBD was found only in non-caveolae/lipid rafts (Fig. 5A). We verified the expression of both ecSOD and ecSOD-ΔHBD in total lysates (Fig. S4A). These indicate that HBD of ecSOD is required for its localization in lipid rafts, and that non-lipid rafts-localized ecSOD and ecSOD-ΔHBD may mainly represent their expression in the intracellular secretory pathway before secretion to the extracellular space. We also confirmed that endogenous ecSOD is found in caveolae/lipid rafts in mouse lung tissue which highly expresses ecSOD (Fig. S4B). Figure 5B shows that ecSOD overexpression selectively enhanced VEGF-induced VEGFR2 phosphorylation in caveolae/lipid rafts, but not non-caveolae/lipid rafts. Disruption of caveolae/lipid rafts by pretreatment with cholesterol-binding agent, methyl-β-cyclodextrin (MβCD) [19,39], enhanced VEGF-induced VEGFR2 tyrosine phosphorylation, but completely inhibited ecSOD effects (Fig. S5). These suggest that ecSOD-induced augmentation of VEGFR2 activation is dependent on integrity of caveolae/lipid rafts.

PTPs inhibition prevents ecSOD-induced enhancement of VEGF-induced VEGFR2 autophosphorylation. To determine the mechanism by which ecSOD enhances VEGFR2 autophosphorylation, we examined whether ecSOD-derived H_2O_2 may inactivate PTPs such as DEP-1 and PTP1B, which negatively regulate VEGFR2 activation [24,25]. Figure 6 shows that inhibition of PTPs by sodium orthovanadate (SOV) (Fig. 6A); or knockdown of either DEP-1 or PTP1B, or both proteins with siRNAs (Fig. 6B), significantly enhanced VEGF-induced VEGFR2-pY in LacZ infected cells. Either SOV or double knockdown of DEP1 and PTP1B almost completely prevented ecSOD-induced enhancement of VEGFR2 phosphorylation (Fig. 6A and 6B), while either DEP-1 siRNA or PTP1B siRNA alone partially but significantly blocked ecSOD effects. All these treatments had no effects on basal VEGFR2 phosphorylation (data not shown). These results suggest that ecSOD-induced enhancement of VEGF-induced VEGFR2-pY is mediated at least through inhibition of DEP-1 and/or PTP1B.

ecSOD induces oxidative inactivation of DEP1 and PTP1B localized in caveolae/lipid rafts

Since PTPs are inactivated by ROS via reactive Cys oxidation [4,5], we next examined whether DEP1 and PTP1B are localized in caveolin-enriched lipid rafts, and oxidized by ecSOD. Figure 7A shows that both DEP1 and PTP1B are found in both

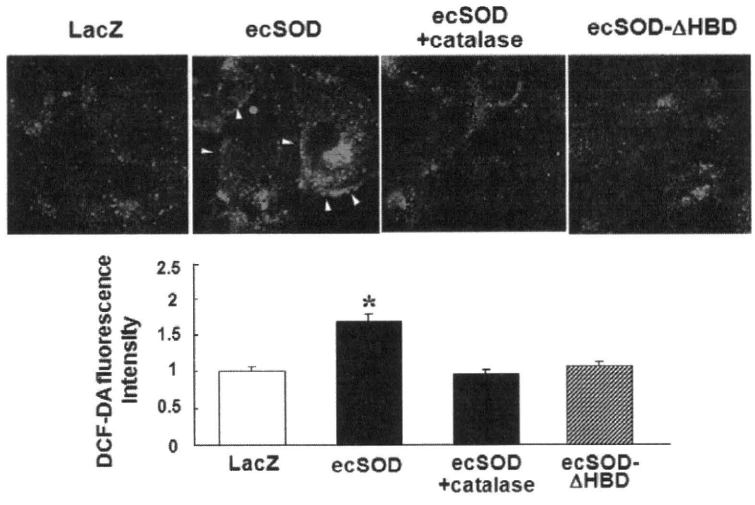

Figure 4. ecSOD increases H_2O_2 levels, in a HBD-dependent manner, in ECs. DCF fluorescence was measured by confocal microscopy in HUVECs infected with Ad.LacZ, Ad.ecSOD pretreated with or without catalase (500 U/ml, for 1 hr), or Ad.ecSOD-ΔHBD. Arrows indicate plasma membrane DCF staining. Lower panel shows the average of DCF fluorescence at 4 different fields (×63) (n = 4). * $p<0.05$ vs. Ad.LacZ.
doi:10.1371/journal.pone.0010189.g004

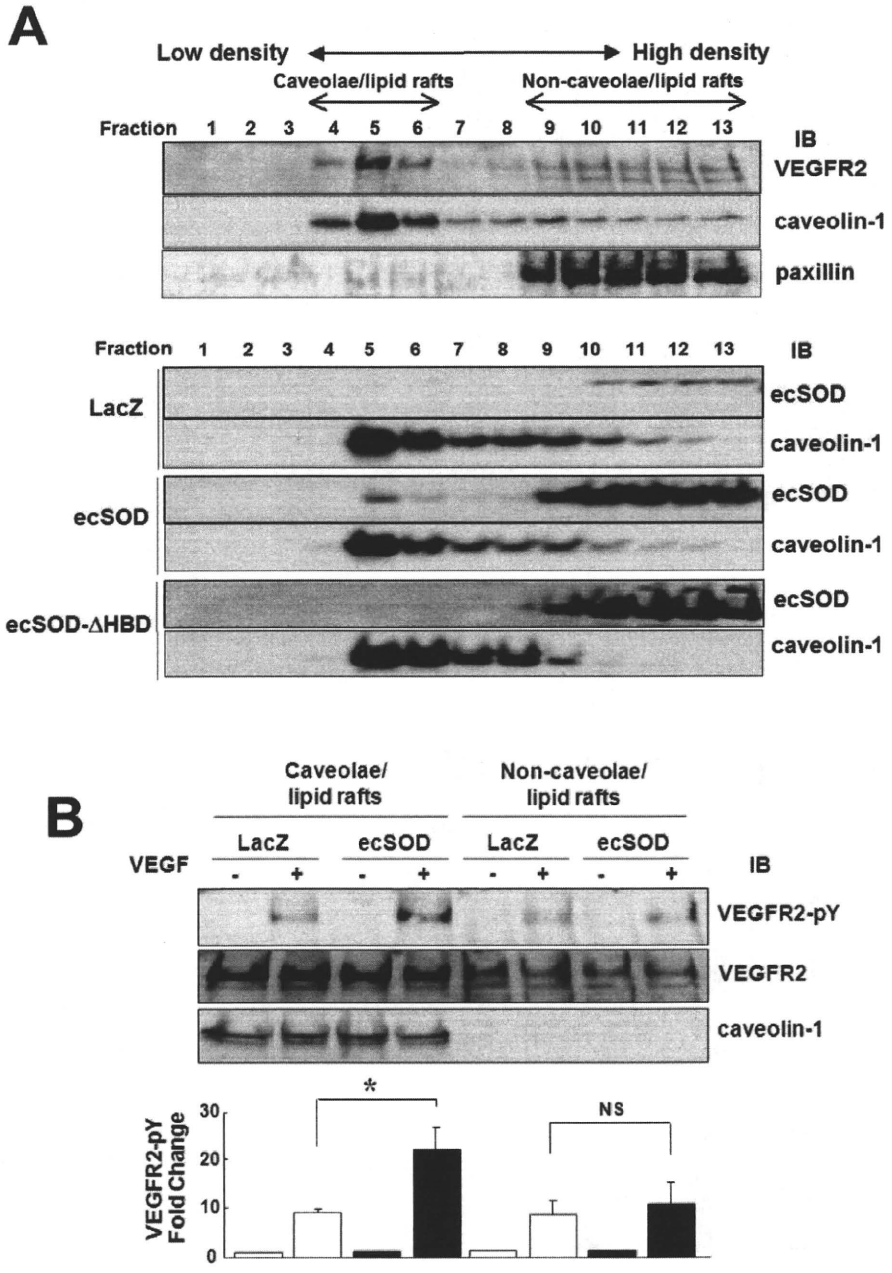

Figure 5. ecSOD localized in caveolae/lipid rafts via HBD enhances VEGF-induced VEGFR2 autophoshorylation in these microdomains. A. After sucrose gradient centrifugation to isolate caveolae/lipid rafts, equal volume of each fraction from top to bottom (total 13 fractions) was IB with anti-VEGFR2, caveolin-1, or paxillin Abs (upper panel). In lower panel, Ad.LacZ or Ad.ecSOD or Ad.ecSOD-ΔHBD-infected HUVECs were used for caveolae/lipid rafts isolation, and each fraction was IB with anti-ecSOD or caveolin-1 Abs. **B.** Ad.LacZ or Ad.ecSOD-infected HUVECs were stimulated with VEGF (20 ng/ml) for 5 min, and followed by caveolae/lipid rafts fractionation. Equal amounts of proteins from pooled Fraction 4–6 (caveolae/lipid rafts) and Fraction 9–13 (non-caveolae/lipid rafts) were IB with anti-VEGFR2-pY1175, total VEGFR2 or caveolin-1 Abs (n = 3). *$p<0.05$.

doi:10.1371/journal.pone.0010189.g005

caveolae/lipid rafts and non-caveolae/lipid rafts fractions, and that ecSOD overexpression decreased their PTP activity in caveolae/lipid rafts, but not non-caveolae/lipid rafts (Fig. 7B). Furthermore, newly-developed Cys-SOH trapping reagent [36] revealed that Ad.ecSOD increased Cys-OH formation of DEP1 and PTP1B in lipid rafts fraction. These suggest that extracellular H_2O_2 generated by ecSOD induces oxidative inactivation of DEP1/PTP1B in caveolae/lipid rafts, thereby promoting VEGF-induced VEGFR2 autophosphorylation in these specialized microdomains.

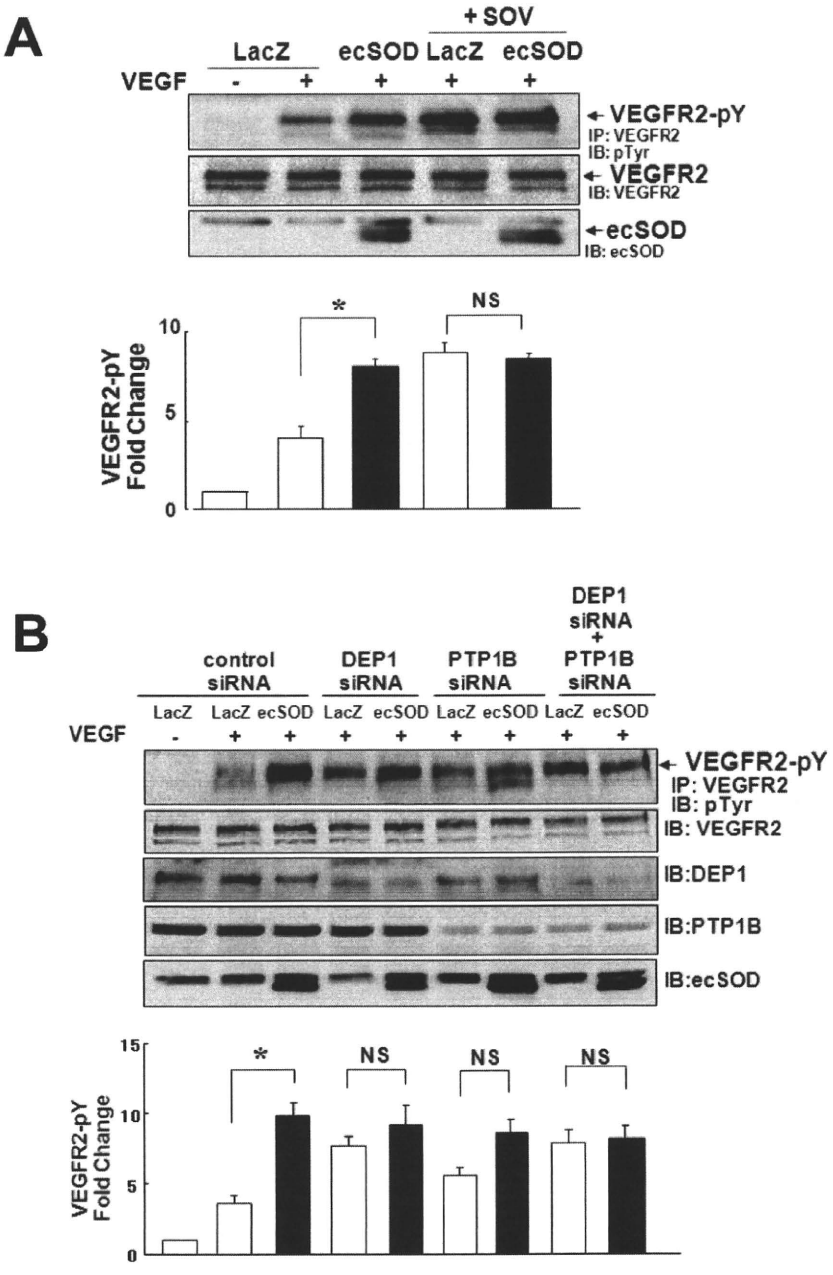

Figure 6. Inhibition of PTPs or knockdown of DEP1 and PTP1B prevents ecSOD-induced enhancement of VEGFR2 autophosphorylation. A. HUVECs infected with Ad.LacZ or Ad.ecSOD were pretreated with 0.3 mM sodium orthovanadate (SOV) for 30 min, and stimulated with VEGF (20 ng/ml) for 5 min. Lysates were used for measurement of VEGFR2-pY or total VEGFR2 or ecSOD expression (n = 3). **B.** HUVECs were transfected with DEP1 or/and PTP1B siRNA, and then infected Ad.LacZ or Ad.ecSOD. Cells were stimulated with VEGF (20 ng/ml) for 5 min and lysates were used for measurement of VEGFR2-pY and expression of proteins indicated (n = 4). * $p<0.05$.
doi:10.1371/journal.pone.0010189.g006

ecSOD promotes VEGF-induced EC migration

We next examined the functional consequence of enhancement of VEGFR2 activation by ecSOD-derived extracellular H_2O_2 in VEGF-induced EC migration and proliferation. Figure 8 using modified Boyden chamber assay shows that ecSOD, but not ecSOD-ΔHBD, significantly enhanced VEGF-induced migration without affecting sphingosine-1-phosphate (S1P)-induced response. Thus, ecSOD-induced effect is specific for VEGFR2 signaling. Importantly, ecSOD-induced enhancement of VEGF-induced EC migration was prevented by catalase, supporting the role of ecSOD-derived H_2O_2. VEGF-induced EC proliferation was also augmented by Ad.ecSOD (Fig. S6). These effects of ecSOD were associated with an enhancement of VEGFR2 downstream signaling such as PLCγ and p38MAPK phosphorylation (Fig. S7).

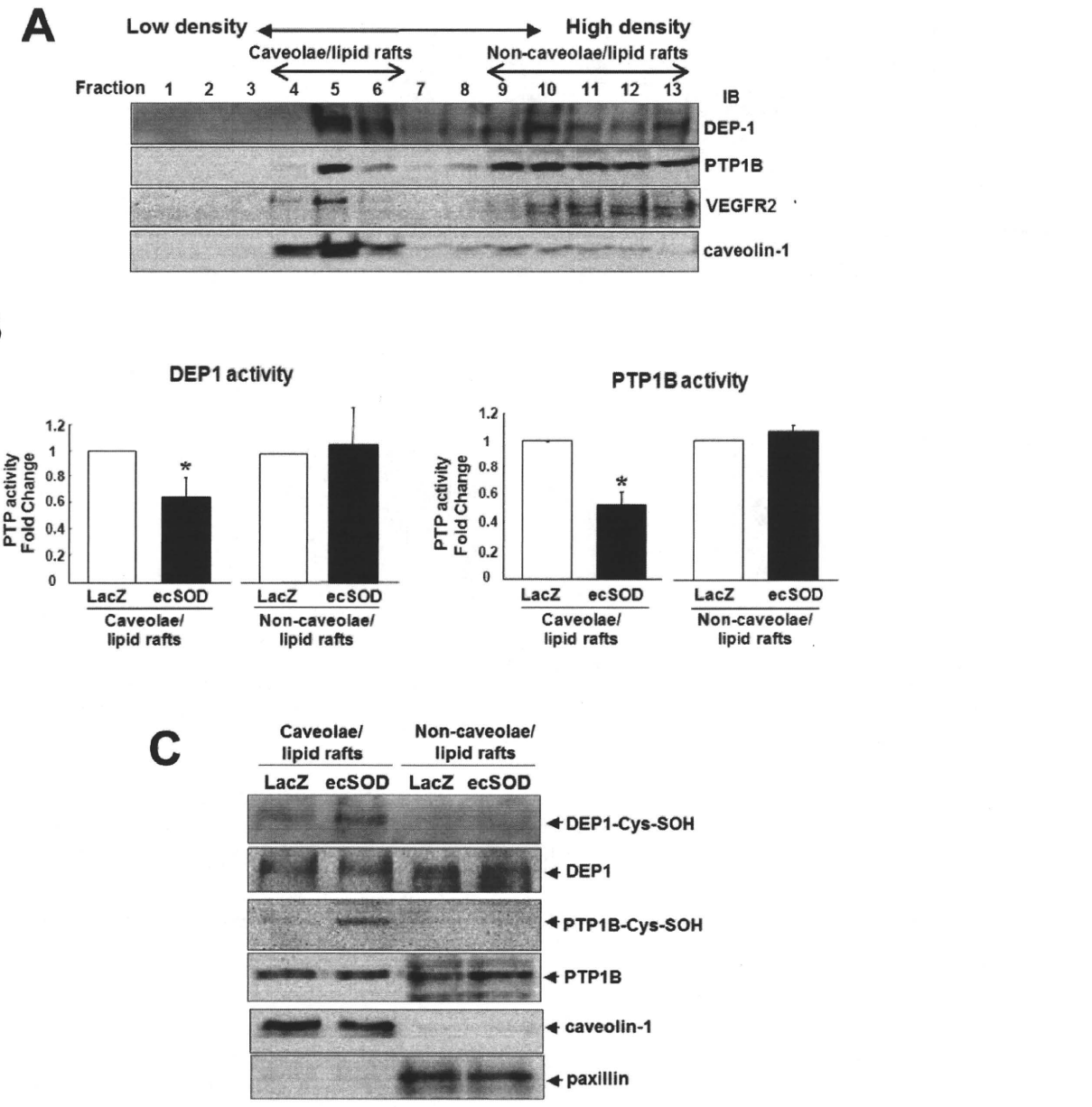

Figure 7. ecSOD induces inactivation and oxidation of DEP-1 and PTP1B localized in caveolae/lipid rafts. A. After sucrose gradient centrifugation, equal volumes of each fraction from top to bottom (total 13 fractions) were IB with anti-DEP-1, PTP1B, VEGFR2 or caveolin-1 Abs. **B.** DEP-1 and PTP1B activities in pooled Fraction 4–6 (caveolae/lipid rafts) and Fraction 9–13 (non-caveolae/lipid rafts) in Ad.LacZ and Ad.ecSOD-infected HUVECs were measured using pNPP as a substrate after IP with anti-DEP-1, PTP1B Abs. The values were expressed as a ratio to Ad.LacZ infected PTP activity (defined as 1.0) in each fraction (n = 3) *$p<0.05$. **C.** Ad.LacZ or Ad.ecSOD-infected HUVECs were extracted in the presence of biotin-labeled Cys-SOH trapping reagent DCP-Bio1. After sucrose gradient centrifugation, pooled Fraction 4–6 and Fraction 9–13 were affinity captured with streptavidin beads to purify the Cys-SOH formed protein, followed by IB with anti-DEP-1 or PTP1B Abs.
doi:10.1371/journal.pone.0010189.g007

Discussion

The present study provides novel evidence that ecSOD functions as a generator of extracellular H_2O_2 in specific subcellular compartments to promote VEGF signaling linked to angiogenesis. Here we show that: 1) gene transfer of ecSOD, but not ecSOD-ΔHBD, increases H_2O_2 levels in adductor muscle, and promotes angiogenesis in response to hindlimb ischemia; 2) H_2O_2 levels in both non-ischemic and ischemic hindlimbs are markedly reduced in ecSOD$^{-/-}$ mice; 3) *In vitro*, overexpression of ecSOD, but not ecSOD-ΔHBD, in cultured medium in ECs enhances VEGF-induced VEGFR2-pY through generation of extracellular H_2O_2; 4) HBD of ecSOD is required for localization of ecSOD at plasma membrane caveolin-enriched lipid rafts where VEGFR2

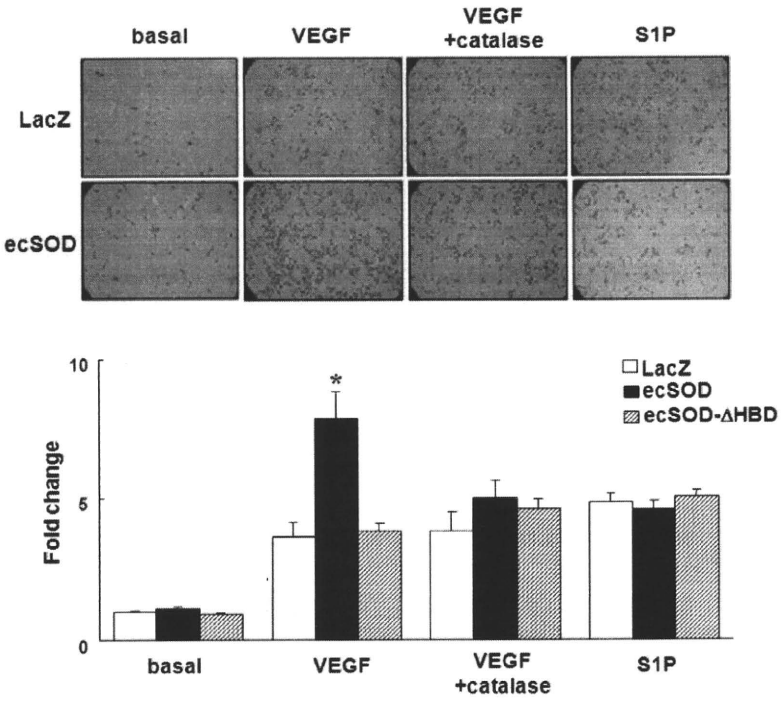

Figure 8. ecSOD promotes VEGF-induced EC migration in a HBD-dependent manner. HUVECs infected with Ad.LacZ or Ad.ecSOD or Ad.ecSOD-ΔHBD were stimulated with 20 ng/ml VEGF or 10 μmol/L sphingosine-1-phosphate (S1P) for 6 hours, and cell migration was measured by the modified Boyden chamber method. Some cells were pretreated with 500 U/ml catalase for 15 min and performed migration assay in the presence of catalase. Bar graph represents averaged data, expressed as cell number counted per 10 fields (x200) and fold change over that in unstimulated cells (control). * $p<0.05$ vs. Ad.LacZ+VEGF.
doi:10.1371/journal.pone.0010189.g008

and PTP1B/DEP-1 are found; 5) endogenous ecSOD is also found in caveolae/lipid rafts in tissues enriched with ecSOD; 6) VEGF-induced VEGFR2-pY in caveolae/lipid rafts, but not non-lipid rafts, is selectively enhanced by ecSOD, which is at least due to oxidative inactivation of PTP1B and DEP1 in caveolae/lipid rafts; 7) ecSOD-derived H_2O_2 promotes VEGF-induced EC migration in a HBD-dependent manner.

Exogenous H_2O_2 can increase angiogenic gene expression and promote pro-angiogenesis responses in ECs [8,13]. However, since H_2O_2 is diffusible and short-lived, its application for therapeutic neovascularization *in vivo* is difficult and not efficient. ecSOD is the enzyme that catalyzes dismutation of O_2^- to produce H_2O_2 in the extracellular space by anchoring to ECs surface or extracellular matrix through HBD [14]. We previously reported that ecSOD expression is increased in response to hindlimb ischemia, and that post-ischemic revascularization is impaired in ecSOD$^{-/-}$ mice [17]. However, a role of ecSOD-derived H_2O_2 in VEGF signaling and ischemia-induced angiogenesis was virtually unexplored. Here we show that gene transfer of Ad.ecSOD, but not Ad.ecSOD-ΔHBD, increases H_2O_2 production in adductor muscles, as measured by Amplex Red assay, which predominantly detects extracellular H_2O_2, as well as promotes blood flow recovery and capillary formation in response to hindlimb ischemia. Furthermore, ecSOD$^{-/-}$ mice show significant reduction of H_2O_2 levels in both non-ischemic and ischemic hindlimbs. These results strongly suggest that ecSOD bound to tissue via HBD plays an important to role as a generator of extracellular H_2O_2 to promote angiogenesis *in vivo*. To determine the underlying mechanisms, we examined the effects of ecSOD-derived H_2O_2 on VEGF signaling in ECs. The present study demonstrates for the first time that overexpression of ecSOD, but not ecSOD-ΔHBD, in ECs or its conditioned media enhances VEGF-induced VEGFR2 autophosphorylation. Moreover, these ecSOD-induced effects on VEGFR2, but not VEGF-induced VEGFR2 autophosphorylation, are inhibited by short-term pretreatment with catalase that scavenges extracellular H_2O_2. Thus, these findings indicate that extracellular H_2O_2 derived from ecSOD promotes VEGF-induced VEGFR2-pY in ECs in a HBD-dependent manner.

In this study, we found that H_2O_2 concentration in culture media of Ad.ecSOD-infected ECs is around 1 μM, while exogenous H_2O_2 requires at least 500 μM to enhance VEGF-induced receptor phosphorylation. These results support the possibility that ecSOD binding to ECs surface via HBD may provide the microenvironment in which extracellular H_2O_2 generated by ecSOD is more compartmentalized than exogenously-applied H_2O_2. Of note, either high concentration of exogenous H_2O_2 or Ad.ecSOD has no effects on basal VEGFR2-pY. These suggest that ligand-induced pre-assembly of VEGFR2 containing signaling complexes and/or their specific localization might be required for promoting effect of extracellular H_2O_2 derived from ECs-bound ecSOD on VEGFR2-pY. It has been shown that VEGF-induced VEGFR2 autophosphorylation is regulated by "intracellular" H_2O_2 derived from Nox2-based NADPH oxidase in ECs [7,8]. NADPH oxidase-dependent O_2^- production occurs both intracellularly and extracellularly [12,40]. Thus, NADPH oxidase-derived O_2^- produced extracellularly may be rapidly dismutated by ecSOD to generate H_2O_2 in close proximity to the VEGFR2 to facilitate its phosphorylation efficiently. Of note,

classical role of ecSOD is to scavenge O_2^- to increase NO bioactivity; however, NO donor has no effect on VEGF-induced phosphorylation of the VEGFR2. Thus, it is H_2O_2 rather than NO, which mediates ecSOD-induced augmentation of VEGFR2 activation in ECs.

ecSOD binds to cell surface HSPGs via HBD, and some cell surface core proteins of HSPGs are localized in caveolae/lipid rafts in ECs [28,41]. We thus examined whether ecSOD-induced modulation of VEGFR2 might occur in these specialized microdomains. Sucrose gradient fractionation reveals that ecSOD is localized in both caveolae/lipid rafts and non-caveolae/lipid rafts fractions in Ad.ecSOD-infected ECs, while ecSOD-ΔHBD is found only in non-caveolae/lipid rafts fraction. Of note, endogenous ecSOD protein is also found in caveolae/lipid rafts in lung tissue in which ecSOD is abundantly expressed. We show that VEGF-induced VEGFR2-pY in caveolae/lipid rafts, but not in non-caveolae/lipid rafts, is enhanced by ecSOD. Disruption of caveolae/lipid rafts by cholesterol-binding reagent increases VEGF-induced VEGFR2 autophosphorylation, but prevents ecSOD-induced effect. Mechanism by which cholesterol depletion increases VEGF-induced phosphorylation of VEGFR2 in ECs seems to be due to dissociation of VEGFR2 from caveolin [19]. Thus, these results suggest that ecSOD localization at caveolin-enriched lipid rafts via HBD is required for ecSOD-induced enhancement of ligand-induced VEGFR2 phosphorylation in these specific plasma membrane compartments.

Reversible oxidative inactivation of PTPs by ROS [42,43,44] and their specific localization are important for ROS to increase tyrosine phosphorylation signaling events [4,5]. The initial product of Cys oxidation is Cys-SOH, a key intermediate involved in redox signaling [45]. The present study shows that inhibition of PTPs or knockdown of DEP-1 and/or PTP1B increases VEGF-induced VEGFR2-pY, which prevents ecSOD-induced effect on VEGFR2. These suggest that both DEP1 and PTP1B function as a negative regulator for VEGFR2-pY, as reported previously [24,25], and that ecSOD-derived H_2O_2 inhibits their PTPs activity to promote VEGFR2 phosphorylation. Intriguingly, we found that both DEP1 and PTP1B are localized in both caveolae/lipid rafts and non-lipid rafts in ECs. Moreover, newly-developed cell permeable Cys-SOH trapping probe [36,37] reveals that ecSOD increases Cys-SOH formation of DEP-1 and PTP1B as well as decreases their PTP activity in caveolin-enriched lipid rafts, but not in non-lipid rafts. NADPH oxidase is localized in lipid rafts to generate O_2^- in ECs [21]. These suggest that extracellular H_2O_2 generated by ecSOD locally oxidizes and inactivates DEP-1 and/or PTP1B in caveolae/lipid rafts where NADPH oxidase and VEGFR2 are found, which in turn promotes VEGF-induced VEGFR2 phosphorylation in these specific microdomains. Other possible PTPs that are regulated by ecSOD cannot be ruled out in the current study.

Functionally, ecSOD, but not ecSOD-ΔHBD, promotes VEGF-induced EC migration *in vitro*, which is prevented by exogenous application of catalase. This is consistent with ecSOD-induced augmentation of ischemia-induced angiogenesis *in vivo*. Of note, S1P-induced migration was not affected by Ad.ecSOD, supporting our conclusion that localizing ecSOD, VEGFR2, and DEP-1/PTP1B in lipid rafts as important mechanism by which ecSOD-derived H_2O_2 enhances VEGFR2 signaling lined to angiogenic responses. We previously reported that ecSOD functions to preserve NO bioactivity by scavenging O_2^- in the ischemic tissues, thereby promoting angiogenesis [17]. Similarly, HBD-dependent protective endothelial function of ecSOD via decreasing extracellular O_2^- has been reported in animal model with hypertension [16]. The R213G polymorphism in the ecSOD gene, which reduces binding to endothelium surface and increases serum ecSOD levels, is associated with increased risk of cardiovascular diseases [46]. The present study uncovers a novel mechanism by which ecSOD promotes endothelial functions such as EC migration and proliferation by generating extracellular H_2O_2 at the specific membrane compartment, and thus facilitating VEGF signaling linked to angiogenesis. In contrast, ecSOD overexpression inhibits, instead of increase, tumor angiogenesis and tumor invasion [47,48]. In pro-oxidant pathological conditions such as atherosclerosis and hypertension, ecSOD seems to be inactivated by H_2O_2 derived from ecSOD due to its peroxidase activity [49,50]. Thus, ecSOD gene transfer effect on angiogenesis

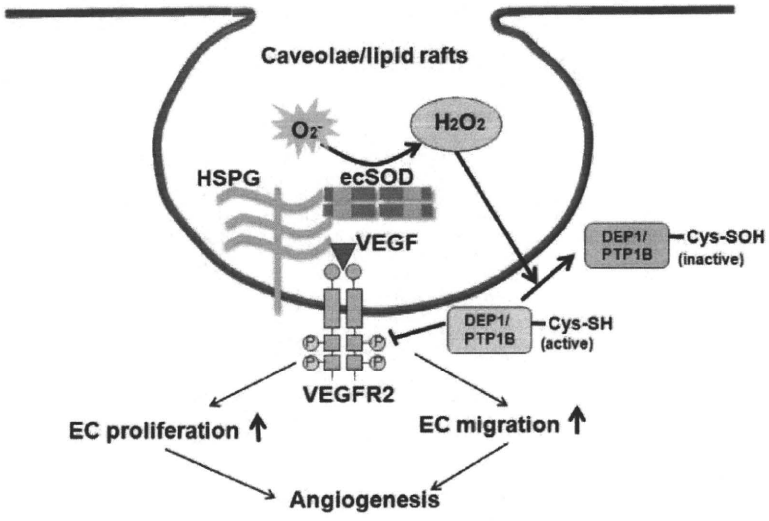

Figure 9. Proposed model for role of ecSOD-derived H_2O_2 in VEGFR2 signaling linked to angiogenesis. Extracellular H_2O_2 generated by ecSOD localized at caveolae/lipid rafts via HBD induces oxidative inactivation of DEP1 and PTP1B in these microdomains, thereby promoting VEGF-induced VEGFR2 phosphorylation, which may contribute to EC migration and proliferation *in vitro* as well as angiogenesis *in vivo*.
doi:10.1371/journal.pone.0010189.g009

in vivo seems to be varied with cell types and context specific [17,47,48,51].

In summary, extracellular H_2O_2 generated by ecSOD localized at caveolin-enriched lipid rafts via HBD efficiently facilitates VEGFR2 signaling via oxidative inactivation of DEP-1/PTP1B in these microdomains, which may contribute to promoting postnatal angiogenesis (Fig. 9). Our previous and present studies may uncover novel mechanism whereby increased ecSOD expression in ischemic tissues promotes reparative neovascularization *in vivo*. It is likely that ecSOD may serve as a potent generator of extracellular H_2O_2 in the plasma membrane specific compartments to promote angiogenesis growth factor signaling. The present findings also imply that ecSOD gene transfer may represent an important therapeutic approach for treatment of angiogenesis-dependent diseases including ischemic heart and limb diseases.

Supporting Information

Figure S1 ecSOD and ecSOD-ΔHBD protein expression and activity in culture medium in adenovirus infected HUVECs. Conditioned media obtained from HUVECs infected with Ad.LacZ or Ad.ecSOD or Ad.ecSOD-ΔHBD was used for Western analysis with anti-human ecSOD antibody (A) or measurement of ecSOD activity (B).
Found at: doi:10.1371/journal.pone.0010189.s001 (0.03 MB PDF)

Figure S2 Exogenous H_2O_2 at physiological concentration cannot enhance VEGF-induced VEGFR2 autophosphorylation. HUVECs were pretreated with indicated concentration of H_2O_2 for 15 min, and stimulated with VEGF (20 ng/ml) for 5 min. Lysates were immunoprecipitated (IP) with anti-VEGFR2 Ab and followed by immunoblotted (IB) with anti-pTyr Ab for measurement of VEGFR2-pY (n = 3).
Found at: doi:10.1371/journal.pone.0010189.s002 (0.05 MB PDF)

Figure S3 Exogenous application of NO donor has no effect on VEGF-induced VEGFR2 autophosphorylation. HUVECs were pretreated with indicated concentration of No donor, diethylenetetraamine-NONOate (DETA-NO) for 30 min, and stimulated with VEGF (20 ng/ml) for 5 min. Lysates were used for measurement of VEGFR2-pY.
Found at: doi:10.1371/journal.pone.0010189.s003 (0.05 MB PDF)

Figure S4 Endogenous ecSOD is localized in caveolae/lipid rafts in mouse lung in which ecSOD is highly expressed. A. Total lysates from HUVECs infected Ad.LacZ or Ad.ecSOD or Ad.ecSOD-ΔHBD for caveolae isolation were IB with anti-ecSOD to confirm the expression of ecSOD and ecSOD-ΔHBD. B. Mouse lung (400 mg) was fractionated to isolate caveolae/lipid rafts and IB with anti-mouse ecSOD or caveolin-1 antibodies.
Found at: doi:10.1371/journal.pone.0010189.s004 (0.05 MB PDF)

Figure S5 Intact caveolae/lipid rafts are required for ecSOD-induced enhancement of VEGFR2 autophosphorylation. HUVECs were pretreated with or without 10 mM methyl-β-cyclodextrin (MβCD) for 1 hr, and stimulated with VEGF (20 ng/ml) for 5 min. Lysates were used for measurement of VEGFR2-pY or total VEGFR2 or ecSOD expression (n = 3). * $p<0.05$.
Found at: doi:10.1371/journal.pone.0010189.s005 (0.09 MB PDF)

Figure S6 ecSOD promotes VEGF-induced EC proliferation. Ad.LacZ or Ad.ecSOD-infected HUVECs were cultured in 0.5% FBS containing medium with or without VEGF (20 ng/ml) for 48 hours, and cell number was counted with a hemocytometer (n = 8). * $p<0.05$.
Found at: doi:10.1371/journal.pone.0010189.s006 (0.01 MB PDF)

Figure S7 ecSOD enhances VEGFR2 downstream signaling in HUVECs. Cell lysates from Ad.LacZ and Ad.ecSOD infected HUVECs with or without VEGF stimulation (20 ng/ml, 5 min) were IB with anti-p-PLCγ or PLCγ (A) or p-p38MAPK or p38MAPK (B) antibodies (n = 3). *$p<0.05$
Found at: doi:10.1371/journal.pone.0010189.s007 (0.08 MB PDF)

Author Contributions

Conceived and designed the experiments: JO NK MR TF MUF. Performed the experiments: JO NU HWK. Analyzed the data: JO. Contributed reagents/materials/analysis tools: NU NK MR RM LBP. Wrote the paper: JO TF MUF.

References

1. Matsumoto T, Claesson-Welsh L (2001) VEGF receptor signal transduction. Sci STKE 2001: RE21.
2. Takahashi T, Yamaguchi S, Chida K, Shibuya M (2001) A single autophosphorylation site on KDR/Flk-1 is essential for VEGF-A-dependent activation of PLC-gamma and DNA synthesis in vascular endothelial cells. Embo J 20: 2768–2778.
3. Lamalice L, Houle F, Jourdan G, Huot J (2004) Phosphorylation of tyrosine 1214 on VEGFR2 is required for VEGF-induced activation of Cdc42 upstream of SAPK2/p38. Oncogene 23: 434–445.
4. Finkel T (1999) Signal transduction by reactive oxygen species in non-phagocytic cells. J Leukoc Biol 65: 337–340.
5. Tonks NK (2005) Redox redux: revisiting PTPs and the control of cell signaling. Cell 121: 667–670.
6. Colavitti R, Pani G, Bedogni B, Anzevino R, Borrello S, et al. (2002) Reactive oxygen species as downstream mediators of angiogenic signaling by vascular endothelial growth factor receptor-2/KDR. J Biol Chem 277: 3101–3108.
7. Ushio-Fukai M, Tang Y, Fukai T, Dikalov SI, Ma Y, et al. (2002) Novel role of gp91(phox)-containing NAD(P)H oxidase in vascular endothelial growth factor-induced signaling and angiogenesis. Circ Res 91: 1160–1167.
8. Ushio-Fukai M (2006) Redox signaling in angiogenesis: role of NADPH oxidase. Cardiovasc Res 71: 226–235.
9. Tojo T, Ushio-Fukai M, Yamaoka-Tojo M, Ikeda S, Patrushev NA, et al. (2005) Role of gp91phox (Nox2)-containing NAD(P)H oxidase in angiogenesis in response to hindlimb ischemia. Circulation 111: 2347–2355.
10. Urao N, Inomata H, Razvi M, Kim HW, Wary K, et al. (2008) Role of nox2-based NADPH oxidase in bone marrow and progenitor cell function involved in neovascularization induced by hindlimb ischemia. Circ Res 103: 212–220.
11. Go YM, Park H, Koval M, Orr M, Reed M, et al. (2009) A key role for mitochondria in endothelial signaling by plasma cysteine/cystine redox potential. Free Radic Biol Med.
12. Chaiswing L, Oberley TD (2009) Extracellular/Microenvironmental Redox State. Antioxid Redox Signal.
13. Gonzalez-Pacheco FR, Deudero JJ, Castellanos MC, Castilla MA, Alvarez-Arroyo MV, et al. (2006) Mechanisms of endothelial response to oxidative aggression: protective role of autologous VEGF and induction of VEGFR2 by H2O2. Am J Physiol Heart Circ Physiol 291: H1395–1401.
14. Fukai T, Folz RJ, Landmesser U, Harrison DG (2002) Extracellular superoxide dismutase and cardiovascular disease. Cardiovasc Res 55: 239–249.
15. Marklund SL (1990) Expression of extracellular superoxide dismutase by human cell lines. Biochem J 266: 213–219.
16. Chu Y, Iida S, Lund DD, Weiss RM, DiBona GF, et al. (2003) Gene transfer of extracellular superoxide dismutase reduces arterial pressure in spontaneously hypertensive rats: role of heparin-binding domain. Circ Res 92: 461–468.
17. Kim HW, Lin A, Guldberg RE, Ushio-Fukai M, Fukai T (2007) Essential role of extracellular SOD in reparative neovascularization induced by hindlimb ischemia. Circ Res 101: 409–419.
18. Insel PA, Patel HH (2009) Membrane rafts and caveolae in cardiovascular signaling. Curr Opin Nephrol Hypertens 18: 50–56.

19. Labrecque L, Royal I, Surprenant DS, Patterson C, Gingras D, et al. (2003) Regulation of vascular endothelial growth factor receptor-2 activity by caveolin-1 and plasma membrane cholesterol. Mol Biol Cell 14: 334–347.
20. Ikeda S, Ushio-Fukai M, Zuo L, Tojo T, Dikalov S, et al. (2005) Novel role of ARF6 in vascular endothelial growth factor-induced signaling and angiogenesis. Circ Res 96: 467–475.
21. Ushio-Fukai M (2009) Compartmentalization of redox signaling through NADPH oxidase-derived ROS. Antioxid Redox Signal 11: 1289–1299.
22. Caselli A, Mazzinghi B, Camici G, Manao G, Ramponi G (2002) Some protein tyrosine phosphatases target in part to lipid rafts and interact with caveolin-1. Biochem Biophys Res Commun 296: 692–697.
23. Oshikawa J, Otsu K, Toya Y, Tsunematsu T, Hankins R, et al. (2004) Insulin resistance in skeletal muscles of caveolin-3-null mice. Proc Natl Acad Sci U S A 101: 12670–12675.
24. Nakamura Y, Patrushev N, Inomata H, Mehta D, Urao N, et al. (2008) Role of protein tyrosine phosphatase 1B in vascular endothelial growth factor signaling and cell-cell adhesions in endothelial cells. Circ Res 102: 1182–1191.
25. Grazia Lampugnani M, Zanetti A, Corada M, Takahashi T, Balconi G, et al. (2003) Contact inhibition of VEGF-induced proliferation requires vascular endothelial cadherin, beta-catenin, and the phosphatase DEP-1/CD148. J Cell Biol 161: 793–804.
26. Gitay-Goren H, Soker S, Vlodavsky I, Neufeld G (1992) The binding of vascular endothelial growth factor to its receptors is dependent on cell surface-associated heparin-like molecules. J Biol Chem 267: 6093–6098.
27. Jakobsson L, Kreuger J, Holmborn K, Lundin L, Eriksson I, et al. (2006) Heparan sulfate in trans potentiates VEGFR-mediated angiogenesis. Dev Cell 10: 625–634.
28. Tkachenko E, Simons M (2002) Clustering induces redistribution of syndecan-4 core protein into raft membrane domains. J Biol Chem 277: 19946–19951.
29. Baljinnyam E, Iwatsubo K, Kurotani R, Wang X, Ulucan C, et al. (2009) Epac increases melanoma cell migration by a heparan sulfate-related mechanism. Am J Physiol Cell Physiol 297: C802–813.
30. Mavromatis K, Fukai T, Tate M, Chesler N, Ku DN, et al. (2000) Early effects of arterial hemodynamic conditions on human saphenous veins perfused ex vivo. Arterioscler Thromb Vasc Biol 20: 1889–1895.
31. Fukai T, Galis ZS, Meng XP, Parthasarathy S, Harrison DG (1998) Vascular expression of extracellular superoxide dismutase in atherosclerosis. J Clin Invest 101: 2101–2111.
32. Ushio-Fukai M, Alexander RW, Akers M, Griendling KK (1998) p38 Mitogen-activated protein kinase is a critical component of the redox-sensitive signaling pathways activated by angiotensin II. Role in vascular smooth muscle cell hypertrophy. J Biol Chem 273: 15022–15029.
33. Qin Z, Gongora MC, Ozumi K, Itoh S, Akram K, et al. (2008) Role of Menkes ATPase in angiotensin II-induced hypertension: a key modulator for extracellular superoxide dismutase function. Hypertension 52: 945–951.
34. Song KS, Li S, Okamoto T, Quilliam LA, Sargiacomo M, et al. (1996) Co-purification and direct interaction of Ras with caveolin, an integral membrane protein of caveolae microdomains. Detergent-free purification of caveolae microdomains. J Biol Chem 271: 9690–9697.
35. Yamaoka-Tojo M, Ushio-Fukai M, Hilenski L, Dikalov SI, Chen YE, et al. (2004) IQGAP1, a novel vascular endothelial growth factor receptor binding protein, is involved in reactive oxygen species-dependent endothelial migration and proliferation. Circ Res 95: 276–283.
36. Poole LB, Klomsiri C, Knaggs SA, Furdui CM, Nelson KJ, et al. (2007) Fluorescent and affinity-based tools to detect cysteine sulfenic acid formation in proteins. Bioconjug Chem 18: 2004–2017.
37. Michalek RD, Nelson KJ, Holbrook BC, Yi JS, Stridiron D, et al. (2007) The requirement of reversible cysteine sulfenic acid formation for T cell activation and function. J Immunol 179: 6456–6467.
38. Ikeda S, Yamaoka-Tojo M, Hilenski L, Patrushev NA, Anwar GM, et al. (2005) IQGAP1 regulates reactive oxygen species-dependent endothelial cell migration through interacting with Nox2. Arterioscler Thromb Vasc Biol 25: 2295–2300.
39. Ushio-Fukai M, Hilenski L, Santanam N, Becker PL, Ma Y, et al. (2001) Cholesterol depletion inhibits epidermal growth factor receptor transactivation by angiotensin II in vascular smooth muscle cells: Role of cholesterol-rich microdomains and focal adhesions in angiotensin II signaling. J Biol Chem 276: 48269–48275.
40. Souchard JP, Barbacanne MA, Margeat E, Maret A, Nepveu F, et al. (1998) Electron spin resonance detection of extracellular superoxide anion released by cultured endothelial cells. Free Radic Res 29: 441–449.
41. Buczek-Thomas JA, Chu CL, Rich CB, Stone PJ, Foster JA, et al. (2002) Heparan sulfate depletion within pulmonary fibroblasts: implications for elastogenesis and repair. J Cell Physiol 192: 294–303.
42. Rhee SG, Bae YS, Lee SR, Kwon J (2000) Hydrogen peroxide: a key messenger that modulates protein phosphorylation through cysteine oxidation. Sci STKE 2000: PE1.
43. Ostman A, Bohmer FD (2001) Regulation of receptor tyrosine kinase signaling by protein tyrosine phosphatases. Trends Cell Biol 11: 258–266.
44. Chiarugi P, Cirri P (2003) Redox regulation of protein tyrosine phosphatases during receptor tyrosine kinase signal transduction. Trends Biochem Sci 28: 509–514.
45. Poole LB, Nelson KJ (2008) Discovering mechanisms of signaling-mediated cysteine oxidation. Curr Opin Chem Biol 12: 18–24.
46. Juul K, Tybjaerg-Hansen A, Marklund S, Heegaard NH, Steffensen R, et al. (2004) Genetically reduced antioxidative protection and increased ischemic heart disease risk: The Copenhagen City Heart Study. Circulation 109: 59–65.
47. Wheeler MD, Smutney OM, Samulski RJ (2003) Secretion of extracellular superoxide dismutase from muscle transduced with recombinant adenovirus inhibits the growth of B16 melanomas in mice. Mol Cancer Res 1: 871–881.
48. Chaiswing L, Zhong W, Cullen JJ, Oberley LW, Oberley TD (2008) Extracellular redox state regulates features associated with prostate cancer cell invasion. Cancer Res 68: 5820–5826.
49. Hink HU, Santanam N, Dikalov S, McCann L, Nguyen AD, et al. (2002) Peroxidase properties of extracellular superoxide dismutase: role of uric acid in modulating in vivo activity. Arterioscler Thromb Vasc Biol 22: 1402–1408.
50. Jung O, Marklund SL, Xia N, Busse R, Brandes RP (2007) Inactivation of extracellular superoxide dismutase contributes to the development of high-volume hypertension. Arterioscler Thromb Vasc Biol 27: 470–477.
51. Laurila JP, Castellone MD, Curcio A, Laatikainen LE, Haaparanta-Solin M, et al. (2009) Extracellular superoxide dismutase is a growth regulatory mediator of tissue injury recovery. Mol Ther 17: 448–454.

Unexpected Role of the Copper Transporter ATP7A in PDGF-Induced Vascular Smooth Muscle Cell Migration

Takashi Ashino, Varadarajan Sudhahar, Norifumi Urao, Jin Oshikawa, Gin-Fu Chen, Huan Wang, Yuqing Huo, Lydia Finney, Stefan Vogt, Ronald D. McKinney, Edward B. Maryon, Jack H. Kaplan, Masuko Ushio-Fukai, Tohru Fukai

Rationale: **Copper, an essential nutrient, has been implicated in vascular remodeling and atherosclerosis with unknown mechanism. Bioavailability of intracellular copper is regulated not only by the copper importer CTR1 (copper transporter 1) but also by the copper exporter ATP7A (Menkes ATPase), whose function is achieved through copper-dependent translocation from *trans*-Golgi network (TGN). Platelet-derived growth factor (PDGF) promotes vascular smooth muscle cell (VSMC) migration, a key component of neointimal formation.**

Objective: **To determine the role of copper transporter ATP7A in PDGF-induced VSMC migration.**

Methods and Results: **Depletion of ATP7A inhibited VSMC migration in response to PDGF or wound scratch in a CTR1/copper-dependent manner. PDGF stimulation promoted ATP7A translocation from the TGN to lipid rafts, which localized at the leading edge, where it colocalized with PDGF receptor and Rac1, in migrating VSMCs. Mechanistically, ATP7A small interfering RNA or CTR small interfering RNA prevented PDGF-induced Rac1 translocation to the leading edge, thereby inhibiting lamellipodia formation. In addition, ATP7A depletion prevented a PDGF-induced decrease in copper level and secretory copper enzyme precursor prolysyl oxidase (Pro-LOX) in lipid raft fraction, as well as PDGF-induced increase in LOX activity. In vivo, ATP7A expression was markedly increased and copper accumulation was observed by synchrotron-based x-ray fluorescence microscopy at neointimal VSMCs in wire injury model.**

Conclusions: **These findings suggest that ATP7A plays an important role in copper-dependent PDGF-stimulated VSMC migration via recruiting Rac1 to lipid rafts at the leading edge, as well as regulating LOX activity. This may contribute to neointimal formation after vascular injury. Our findings provide insight into ATP7A as a novel therapeutic target for vascular remodeling and atherosclerosis. (*Circ Res.* 2010;107:787-799.)**

Key Words: vascular remodeling ■ vascular smooth muscle ■ migration ■ copper transporter ■ platelet-derived growth factor

Copper, an essential micronutrient, plays an important role in physiological repair processes including wound healing and angiogenesis, as well as various pathophysiologies including tumor growth, neurodegenerative disease, and atherosclerosis.[1–7] Copper levels are significantly increased in cancer and atherosclerotic lesions.[8,9] Implanting a copper cuff promotes neointima thickening in response to vascular injury,[10] whereas copper chelators prevent this response[11] and tumor growth.[3] Underlying molecular mechanisms remain unclear. Platelet-derived growth factor (PDGF) is a key growth factor to promote neointimal formation and vascular remodeling in vivo primarily through the PDGF receptor-β (PDGFR) expressed in vascular smooth muscle cells (VSMCs).[12] VSMC migration is a critical event for the development of atherosclerosis and restenosis after vascular injury.[12] PDGF-induced cell migration is regulated by actin cytoskeleton, Rac1 activation and translocation to the leading edge.[12,13] However, a role for copper in PDGF-induced VSMC migration has not been demonstrated.

Because excess copper is toxic, copper homeostasis is tightly controlled by regulation of copper uptake, transport and excretion.[1,2] Indeed, under physiological conditions, the level of intracellular free copper is extraordinarily restricted.[14] Copper uptake is mainly mediated by the copper transporter (CTR)1 copper importer, which is involved in embryonic development.[1,15] Once copper enters the cell via

Original received February 23, 2010; resubmission received May 30, 2010; revised resubmission received July 8, 2010; accepted July 16, 2010. In June 2010, the average time from submission to first decision for all original research papers submitted to *Circulation Research* was 14.5 days.

From the Departments of Medicine (Section of Cardiology) and Pharmacology, Center for Cardiovascular Research (T.A., V.S., G.-F.C., R.D.M., T.F., R.D.M.); Department of Pharmacology, Center for Lung and Vascular Biology, Center for Cardiovascular Research (N.U., J.O., R.D.M., M.U.-F.); and Department of Biochemistry and Molecular Genetics (E.B.M., J.H.K.), University of Illinois at Chicago; Cardiovascular Division (H.W., Y.H.), Department of Medicine, University of Minnesota, Minneapolis; and Biosciences Division (L.F.) and X-ray Science Division (L.F., S.V.), Argonne National Laboratory, Ill.

Correspondence to Tohru Fukai, MD, PhD, Departments of Medicine (Section of Cardiology) and Pharmacology, Center for Cardiovascular Research, University of Illinois at Chicago, 835 S Wolcott, M/C868, E403 MSB, Chicago, IL 60612. E-mail tfukai@uic.edu

Circulation Research **is available at http://circres.ahajournals.org** **DOI: 10.1161/CIRCRESAHA.110.225334**

Non-standard Abbreviations and Acronyms	
ApoE	apolipoprotein E
ATP7A	Menkes ATPase, copper-transporting P-type ATPase
BCS	bathocuproine disulfonate
CTxB	cholera toxin subunit B
CTR1	copper transporter 1, SLC31A1
ICP-MS	inductively coupled plasma mass spectrometry
LOX	lysyl oxidase
LOX-PP	lysyl oxidase pro-peptide
PDGF	platelet-derived growth factor
PDGFR	platelet-derived growth factor receptor-β
Pro-LOX	proenzyme of lysyl oxidase
HASM	human aortic smooth muscle cell
MASM	mouse aortic smooth muscle cell
RASM	rat aortic smooth muscle cell
siRNA	small interfering RNA
SOD	superoxide dismutase
SXFM	synchrotron-based x-ray fluorescence microscopy
TTM	tetrathiomolybdate
TGN	*trans*-Golgi network
VSMC	vascular smooth muscle cell

CTR1, it can be delivered into various distinct cellular compartments via ATP7A copper transporting ATPase through the Atox1 copper chaperone.[16,17] ATP7A is ubiquitously expressed and transports copper to the extracellular space or to the selected copper enzymes, which are either secreted from cells, or reside within vesicular compartments.[16,17] When intracellular copper increases, ATP7A translocates from *trans*-Golgi network (TGN) to the plasma membrane or to cytoplasmic vesicles,[16,17] thereby maintaining intracellular copper homeostasis and avoiding copper toxicity. This process requires both copper binding to cytoplasmic regions of ATP7A as well as its catalytic turnover.[18,19]

The biological significance of ATP7A in vivo is underscored by Menkes disease, a disorder caused by ATP7A mutations resulting in a marked decrease in copper levels in most tissues except for the kidney and small intestine. Menkes patients show multiple abnormalities secondary to either loss of activity of some secretory copper enzymes or impairment of neuronal activation and other unknown function, leading to death in infancy.[2,20] In vascular tissue, ATP7A is involved in delivering copper to secretory copper enzymes, such as superoxide dismutase (SOD)3 and proenzyme of lysyl oxidase (Pro-LOX).[17,20–22] After secretion, Pro-LOX is processed and activated by proteolysis to a mature active 32-kDa enzyme (LOX) and an 18-kDa propeptide (LOX-PP), both of which are expressed in vascular tissue.[22,23] LOX is known to be critical for vascular extracellular matrix maturation by regulating the cross-linking of collagens or elastin. Of note, LOX is stimulatory but LOX-PP is inhibitory for cell migration.[23–25] No information is available regarding a role of ATP7A in PDGF-mediated vascular migration and remodeling.

Here, we demonstrate the novel role of ATP7A in PDGF-induced VSMC migration. PDGF stimulation promotes ATP7A translocation from the TGN to lipid rafts which localize at the leading edge in migrating VSMC, thereby promoting lamellipodia formation through recruiting Rac1, in a CTR1-dependent manner. This is associated with a decrease in cellular copper and secretory copper enzyme precursor prolysyl oxidase in caveolae/lipid rafts, which may contribute to activation of LOX. In vivo, ATP7A expression is markedly increased and copper accumulation is observed at neointimal VSMC in wire injury model. These findings provide insight into ATP7A as potential therapeutic targets for vascular remodeling and development of atherosclerosis.

Methods

An expanded Methods section is available in the Online Data Supplement at http://circres.ahajournals.org.

Detergent-Free Purification of Caveolin-Rich Membrane Fractions

Caveolae/lipid raft fractions were separated by the sodium carbonate–based detergent-free method.

Copper Measurements

Copper contents were analyzed by inductively coupled plasma mass spectrometry (ICP-MS) using a PlasmaQuad3, as reported previously.[26]

Vascular Injury

Animal protocols were approved by the Animal Care and Use Committee of the University of Illinois at Chicago and University of Minnesota. Wire-induced injury of the carotid artery in apolipoprotein (Apo)E-deficient atherosclerotic mice was performed, as reported previously.[27]

Synchrotron X-Ray Fluorescence Microscopy

Sections (5-μm thick) of formalin-fixed, paraffin-embedded, wire-injured femoral artery were used. For x-ray imaging, the sections (5-μm thick) of formalin-fixed, paraffin-embedded, wire-injured femoral artery were prepared on silicon nitride windows (Silson), as reported previously.[28]

Results

Expression of the ATP7A Copper Transporter and the CTR1 Copper Importer in VSMCs

RT-PCR analysis of rat, mouse, and human aortic smooth muscle cells (RASMs, HASMs, and MASMs) detected both ATP7A and CTR1 expression (Figure 1A). Western analysis with anti-ATP7A antibody showed expression of ATP7A with a 178-kDa protein in whole cell lysates of RASMs, HASMs, and MASMs (Figure 1B).[16,17] By contrast, CTR1 protein was not detected in whole cell lysates, but in caveolae/lipid rafts fraction, by specific anti-CTR1 antibody, as shown later (Figure 5A; Online Figure V, A and B).

ATP7A Is Involved in PDGF-Induced VSMC Migration in a Copper-Dependent Manner

We next examined the role of ATP7A in VSMC migration. Modified Boyden chamber assays demonstrated that knockdown of endogenous ATP7A expression with small interfering (si)RNA significantly inhibited PDGF-stimulated migration in VSMCs (Figure 1C and Online Figure I). Because the

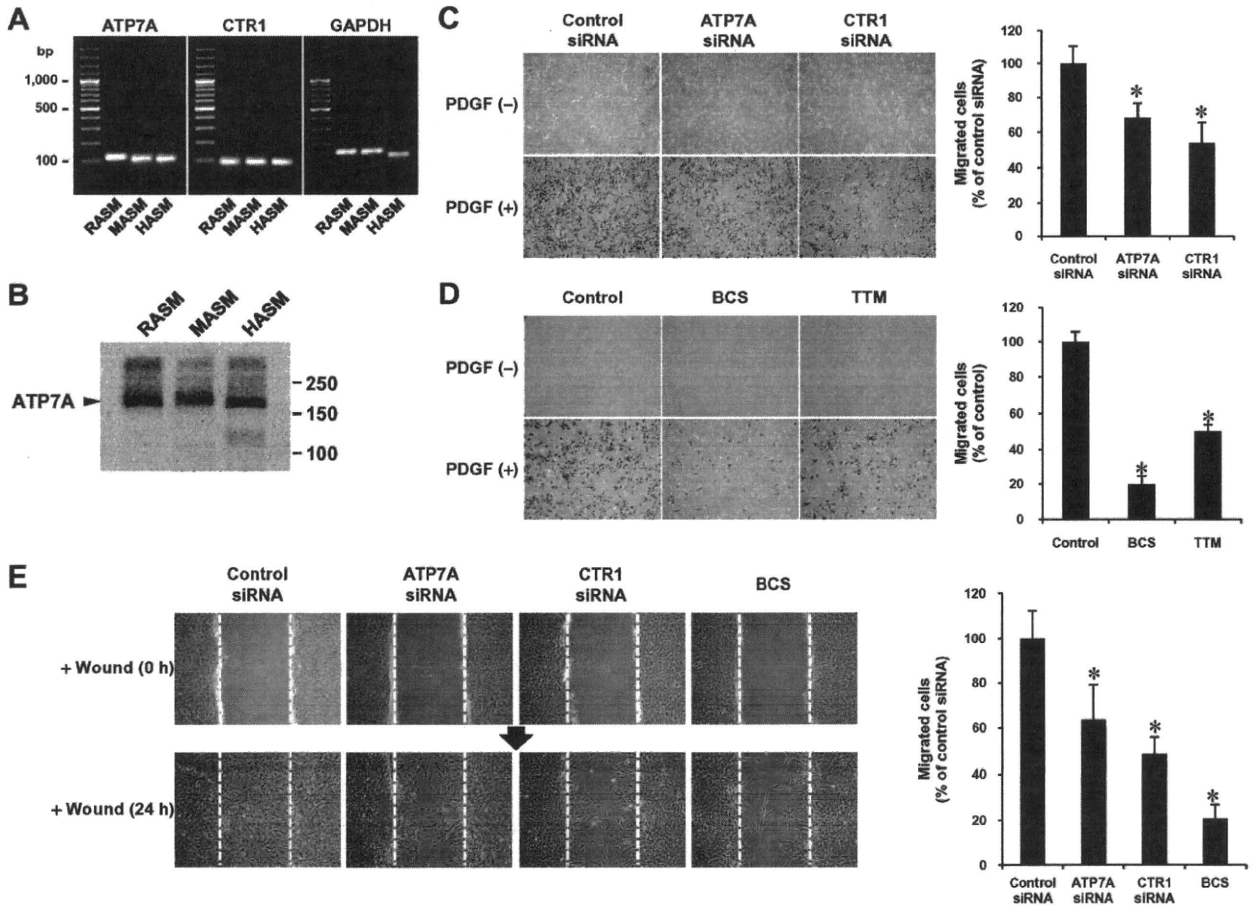

Figure 1. ATP7A is involved in VSMC migration stimulated by PDGF or wound scratch in a copper-dependent manner. A, RT-PCR analysis of ATP7A and CTR1 mRNA expression in various VSMCs (RASMs, HASMs, and MASMs). **B,** Western blot analysis of ATP7A protein expression in various VSMCs. **C and D,** RASMs were transfected with ATP7A, CTR1, or control siRNA for 48 hours or treated with the copper chelator BCS (cell-impermeable) (200 μmol/L for 72 hours) or the copper chelator TTM (cell-permeable) (10 nmol/L for 24 hours). Cell migration was assessed by the modified Boyden chamber assay after stimulation with or without 50 ng/mL PDGF for 8 hours. **E,** Wound-scratch assay was performed in confluent monolayers of RASMs transfected with siRNA or treated with copper chelator in the presence of PDGF (50 ng/mL), as described in the Online Data Supplement. Images were captured immediately after rinsing at 0 hour and at 24 hours after the wounding in the cells. **Bar graph** represents averaged data, expressed as cell number per field. *$P<0.05$ vs control siRNA-treated **(C and E)** or untreated **(D and E)** cells. Values are the means±SD for 3 independent experiments.

copper transporter function of ATP7A is dependent on the delivery of copper from the extracellular space via CTR1,[29,30] we also investigated the role of CTR1. Transfection of VSMCs with CTR1 siRNA significantly reduced endogenous CTR1 expression (Online Figures I [A] and V [B]). PDGF-induced cell migration was significantly inhibited by CTR1 siRNA (Figure 1C) as well as copper chelators tetrathiomolybdate (TTM) (cell-permeable) and bathocuproine disulfonate (BCS) (cell-impermeable) (Figure 1D), suggesting that this response is copper-dependent. Wound scratch assay of confluent monolayer of VSMCs in the presence of PDGF also showed that ATP7A siRNA as well as CTR1 siRNA or BCS significantly inhibited directional cell migration in response to wound injury (Figure 1E). In contrast, transfection of ATP7A siRNA did not have significant effect on PDGF-induced VSMC proliferation (Online Figure II). These results suggest that ATP7A is involved in PDGF-stimulated VSMCs migration in a copper-dependent manner.

PDGF Stimulation Promotes ATP7A Translocation to the Leading Edge in a Copper-Dependent Manner

To gain insight into the mechanism by which ATP7A mediates VSMC migration in response to PDGF, we examined the subcellular localization of ATP7A after wound scratch in the presence of PDGF. In confluent monolayers of VSMC before wounding or in migrating VSMCs away from the scratched area, ATP7A was found predominantly in perinuclear regions (Figure 2A). In contrast, ATP7A accumulated and colocalized with F-actin at the leading edge in actively migrating VSMCs, but did not colocalize with actin stress fibers in the cell body (Figure 2A). We confirmed the specificity of the ATP7A staining by ATP7A siRNA, as shown later (Figure 3D). Furthermore, nonimmune IgG (control) showed no staining (data not shown). Pretreatment of VSMCs with copper chelators BCS or TTM as well as CTR1 siRNA markedly inhibited wound-induced transloca-

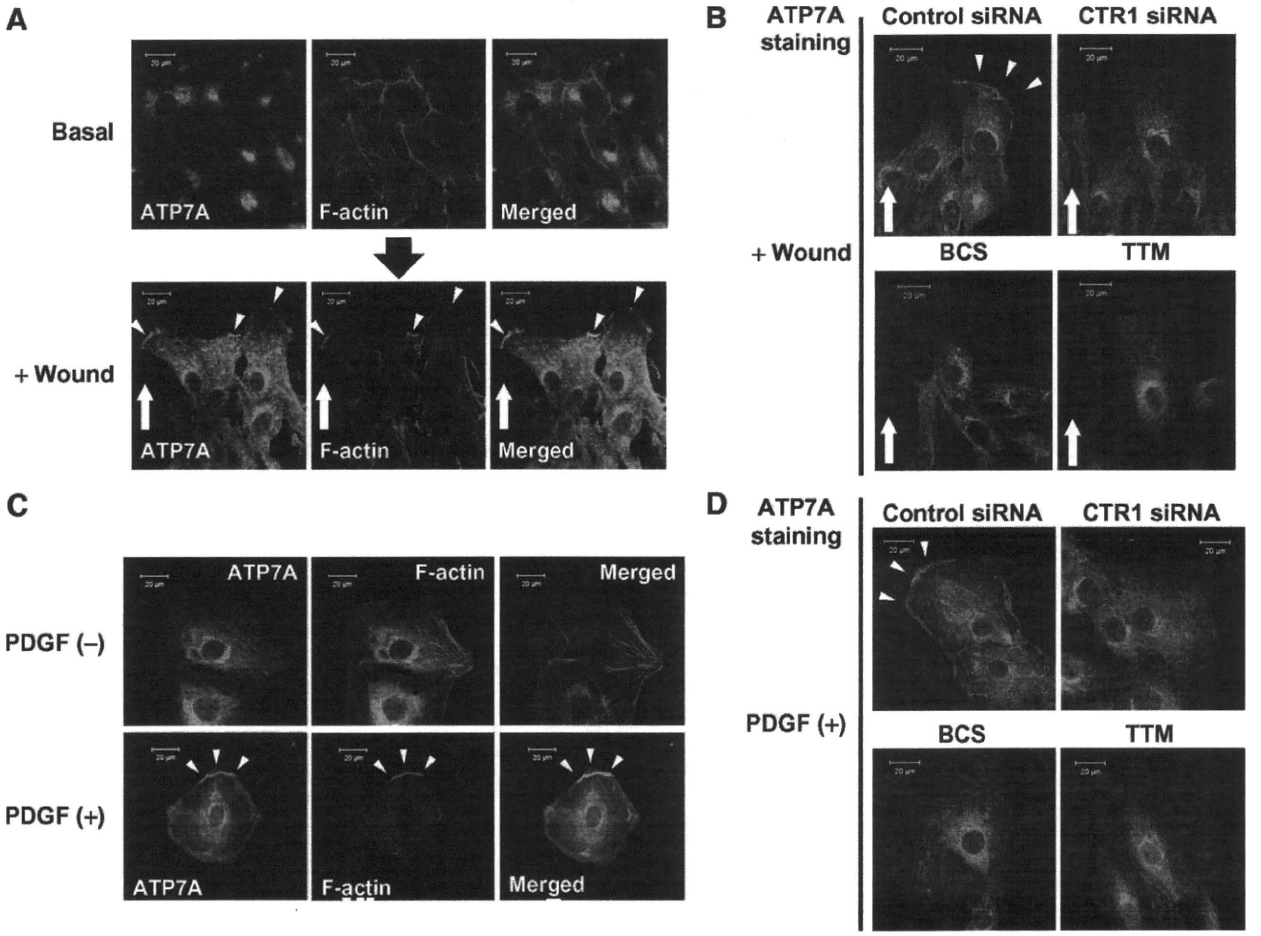

Figure 2. ATP7A is translocated to the leading edge in VSMCs stimulated by wound scratch or PDGF in a copper-dependent manner. A and B, Confluent monolayer of RASMs before **(top)** and after wound scratch in the presence of 50 ng/mL PDGF for 18 hours **(bottom)** were stained with anti-ATP7A **(green)** and Alexa Fluor 568-phalloidin **(red)** antibodies. **Small white arrowheads** point to the leading edge, and **large arrows** point to direction of migration. **C and D,** Growth-arrested RASMs were stimulated with or without 50 ng/mL PDGF for 5 minutes. Cells were costained for ATP7A and phalloidin. In some experiments, RASMs transfected with CTR1, or control siRNA, or treated with copper chelators BCS or TTM were stimulated by wound scratch **(B)** or PDGF **(D)**. Results for **A through D** are representative of 3 independent replicates of immunofluorescence images.

tion of ATP7A toward the leading edge (Figure 2B). Similarly, in untreated VSMC, ATP7A was found predominantly in perinuclear regions, and colocalized with syntaxin 6, a TGN marker (Online Figure III, B). PDGF stimulation rapidly promoted ATP7A translocation from the Golgi to the plasma membrane leading edge with peak at 5 minutes, which gradually returned to the perinuclear region within 30 minutes (Figure 2C; Online Figure III, A). This effect was observed in VSMCs from other species, such as MASMs, suggesting that function of ATP7A is similar in VSMC across the different species (Online Figure III, C). Furthermore, this response was inhibited by copper chelators as well as knockdown of CTR1 (Figure 2D). Of note, the location of syntaxin 6 was not altered by PDGF in VSMCs (Online Figure III, B), suggesting that PDGF-induced ATP7A translocation was not attributable to the general effect on Golgi structure. Taken together, these findings suggest that PDGF stimulation promotes ATP7A translocation to the leading edge, in a copper-dependent manner, thereby stimulating VSMC migration.

ATP7A Is Involved in PDGF-Stimulated Lamellipodia Formation and Rac1 Translocation in a CTR1-Dependent Manner in VSMCs

To assess further the mechanism by which ATP7A is involved in VSMC migration, we examined whether ATP7A is involved in actin reorganization. Knockdown of ATP7A by siRNA significantly impaired wound scratch- (Figure 3A) and PDGF- (Figure 3B) stimulated lamellipodia formation at the leading edge in VSMCs as visualized by phalloidin staining. These effects were also prevented by siRNA knockdown of the CTR1. Because Rac1 plays a role in lamellipodia formation and cell migration,[31] we next examined the role of ATP7A in Rac1 activation and translocation in PDGF-stimulated VSMCs. PDGF stimulation increased active, GTP-bound form of Rac1 within 1 minute, which was not affected by either ATP7A or CTR1 siRNA (Online Figure IV). Immunofluorescence analysis showed that PDGF stimulation promoted translocation of Rac1 to the leading edge where it colocalized with ATP7A (Figure 3C). Coimmuno-

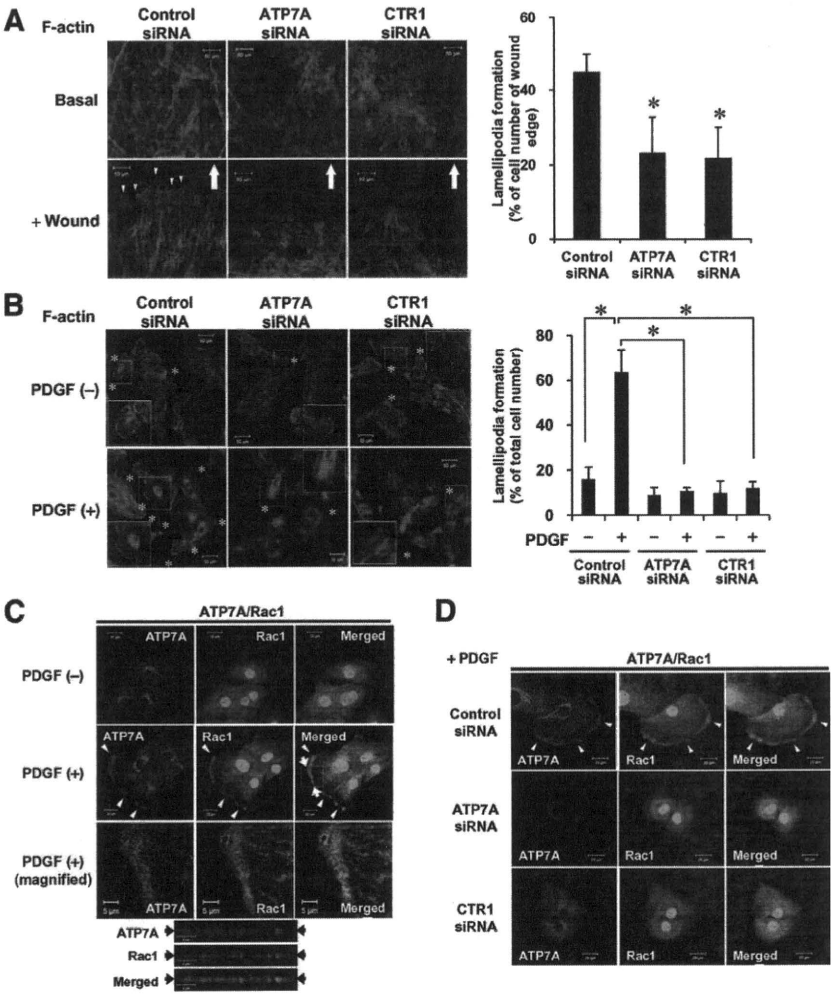

Figure 3. ATP7A is involved in PDGF-stimulated lamellipodia formation and Rac1 translocation in a CTR1-dependent manner in VSMCs. A and B, RASMs transfected with control siRNA or CTR1 siRNA or ATP7A siRNA were stimulated with wound scratch **(A)** or 50 ng/mL PDGF **(B)** as described for Figure 2, and cells were stained for phalloidin to visualize lamellipodia formation. Cells with lamellipodia formation were expressed as percentage of cell number of wound edge **(A)** or total cell number **(B)** (means±SD, n=3). In **B**, cells in boxes are magnified in **insets. Small white arrowheads** point to the leading edge, and **large arrows** point to direction of migration. *$P<0.05$ vs control siRNA-treated cells. **C and D**, RASMs stimulated with or without PDGF as described above and costained with anti-ATP7A antibody **(red)** and anti-Rac1 antibody **(green)**. In **D**, RASMs were transfected with control siRNA or CTR1 siRNA or ATP7A siRNA as described. All fluorescence images were taken at 5 different fields/well, and the cell images are representative of >3 different experiments.

precipitation analysis showed that ATP7A associated with Rac1 in the basal state, which was further enhanced after PDGF stimulation (Online Figure IV, C), suggesting that ATP7A recruits Rac1 to the lipid rafts via binding to Rac1 in response to PDGF directly or indirectly. Furthermore, Rac1 trafficking to the leading edge was inhibited by either ATP7A or CTR1 siRNA (Figure 3D). Thus, the copper transporter ATP7A is involved in PDGF-stimulated translocation of Rac1 to the leading edge, but not Rac1 activation, in a CTR1-dependent manner, which may contribute to lamellipodia formation and VSMC migration.

ATP7A Colocalizes With PDGFR at the Leading Edge in a CTR1-Dependent Manner in PDGF-Stimulated VSMCs

Because we found that ATP7A is a downstream mediator for PDGFR signaling linked to VSMC migration, we next examined the relationship between ATP7A and PDGFR in PDGF-stimulated VSMCs. Immunofluorescence analysis showed that ATP7A colocalized with PDGFR at the leading edge after PDGF stimulation (Figure 4A). Of note, both CTR1 and ATP7A siRNAs inhibited PDGF-induced ATP7A movement to the leading edge without affecting PDGFR localization (Figure 4B). Coimmunoprecipitation analysis further confirmed that PDGF stimulation promoted PDGFR association with ATP7A, which was somewhat inhibited by CTR1 siRNA (Figure 4C). Under this condition, PDGF-induced PDGFR autophosphorylation was not affected by CTR1 siRNA (Figure 4C). Taken together, these results suggest that PDGF stimulation induces colocalization and association of ATP7A with PDGFR at the leading edge in a CTR1-dependent manner, and that CTR1-ATP7A pathway is downstream of PDGFR activation.

PDGF Promotes ATP7A Recruitment to the Caveolae/Lipid Rafts, Where PDGFR, Rac1, and CTR1 Are Localized, in a CTR1-Dependent Manner

To gain further insight into the subcellular compartments in which ATP7A is localized, we performed detergent-free sucrose gradient fractionation in VSMCs, as previously described.[32] Western analysis of sequential fractions from the gradient showed that ATP7A was found in both caveolin-enriched lipid rafts fractions and noncaveolae/lipid rafts fractions which mainly contain paxillin (Figure 5A).[33] By contrast, the CTR1 copper importer was predominantly found in caveolae/lipid rafts. The specificity of the CTR1 antibody, which detects glycosylated CTR1,[34] was verified by CTR1-deficient mouse embryonic fibroblast cells[30] and VSMCs

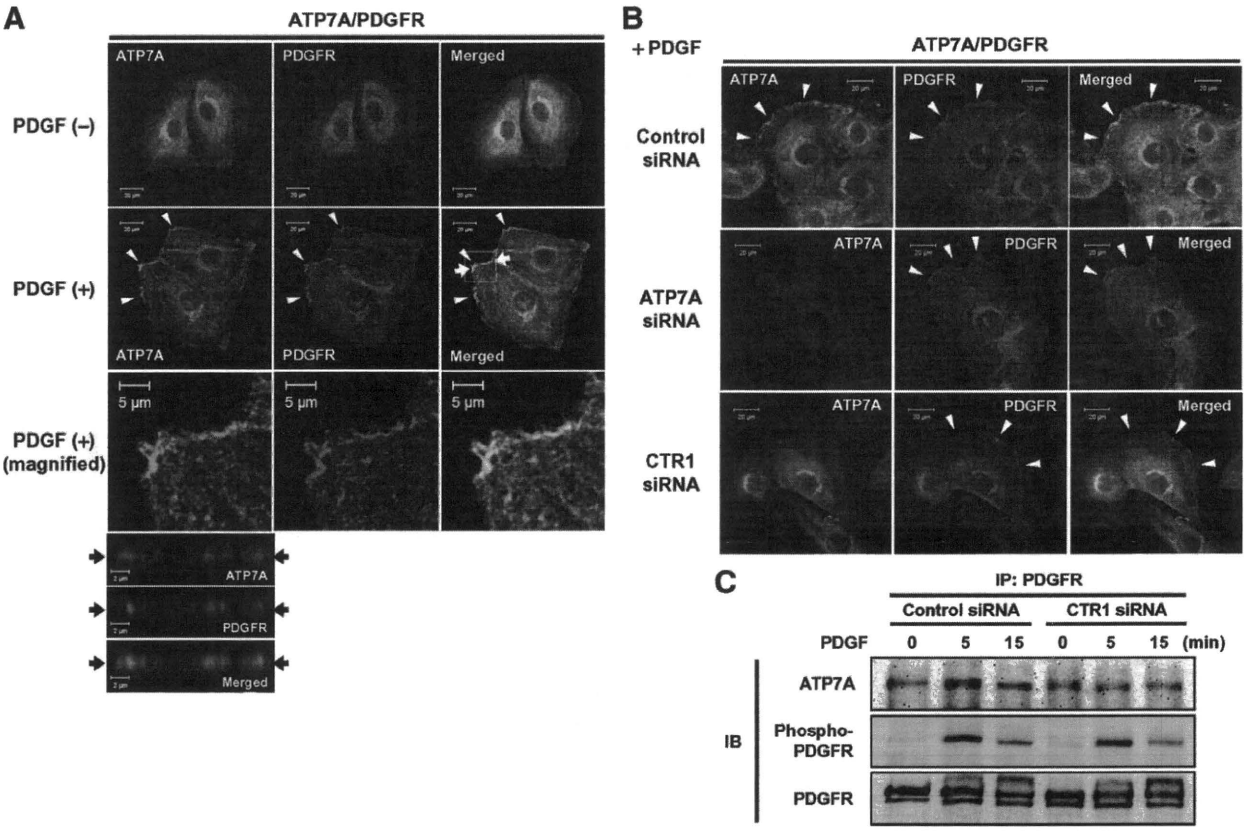

Figure 4. ATP7A colocalizes with PDGFR at the leading edge in a CTR1-dependent manner in PDGF-stimulated VSMCs. A through C, Growth-arrested RASMs were stimulated with 50 ng/mL PDGF for 5 minutes. All fluorescence images were taken at 5 different fields/well, and the cell images are representative of >3 different experiments. **A,** Effect of PDGF on subcellular localization of ATP7A and PDGFR in VSMCs. RASMs were stained with anti-ATP7A antibody **(green)** and anti-PDGFR antibody **(red). B,** Effect of ATP7A or CTR1 siRNA on subcellular localization of ATP7A and PDGFR in PDGF-treated cells. RASMs transfected with CTR1, ATP7A, or control siRNA were double-stained with anti-ATP7A antibody **(green)** and anti-PDGFR antibody **(red). C,** PDGF stimulation promoted PDGFR association with ATP7A in a CTR1-dependent manner. RASMs were transfected with control siRNA or CTR1 siRNA. Growth-arrested confluent monolayer of RASMs was stimulated with 50 ng/mL PDGF for indicated times (min). Lysates were immunoprecipitate (IP) with anti-PDGFR antibody, followed by immunoblot (IB) with ATP7A, phospho-PDGFR, and PDGFR antibody.

transfected with CTR1 siRNA (Online Figure V, A and B). Localization of ATP7A and CTR1 in caveolae/lipid rafts was further confirmed in various VSMCs, including RASM, HASM, and MASM (Online Figure V, C) and using detergent-free OptiPrep gradient cell fractionation (Online Figure V, D). Figure 5B shows that PDGF stimulation for 5 minutes promoted recruitment of ATP7A, CTR1 and Rac1 to the caveolae/lipid rafts fractions without affecting PDGFR localization, which was associated with an increase in PDGFR phosphorylation in these fractions. Significantly, CTR1 siRNA prevented PDGF-induced translocation of ATP7A and Rac1 to the caveolae/lipid rafts without affecting PDGFR phosphorylation (Figure 5B). These suggest that PDGF-induced PDGFR autophosphorylation occurs in caveolae/lipid rafts, which in turn promotes recruitment of ATP7A and Rac1 to these specialized microdomains where PDGFR is localized, in a CTR1-dependent manner.

ATP7A Is Translocated to the Lipid Rafts Localized at the Leading Edge in PDGF-Stimulated VSMCs

Lipid rafts have been shown to be localized at the leading edge during cell migration.[35] We thus examined the spatial relationships among ATP7A, lipid rafts and leading edge after PDGF stimulation using immunofluorescence analysis. As shown in Figure 5C and Online Figure VI (B), ATP7A colocalized with cholera toxin subunit B (CTxB), a lipid raft marker,[35] at the leading edge in PDGF- and wound scratch-stimulated VSMCs. Furthermore, CTxB accumulated and colocalized with F-actin at the leading edge in actively migrating VSMCs (Online Figure VI, A and C). Disruption of lipid rafts by cholesterol binding reagent, methyl-β-cyclodextrin, completely abrogated the ATP7A localization at the leading edge and CTxB staining (Figure 5D) as well as lamellipodia formation (Online Figure VI, A). These results suggest that PDGF stimulates translocation of ATP7A to the lipid rafts localized at the leading edge, thereby promoting lamellipodia formation.

PDGF Stimulation Reduces Copper Content in Caveolae/Lipid Raft Fractions in VSMCs

Because ATP7A is involved in exporting copper to the extracellular space, we next examined the effects of PDGF on copper levels in VSMCs. At first, we performed ^{64}Cu

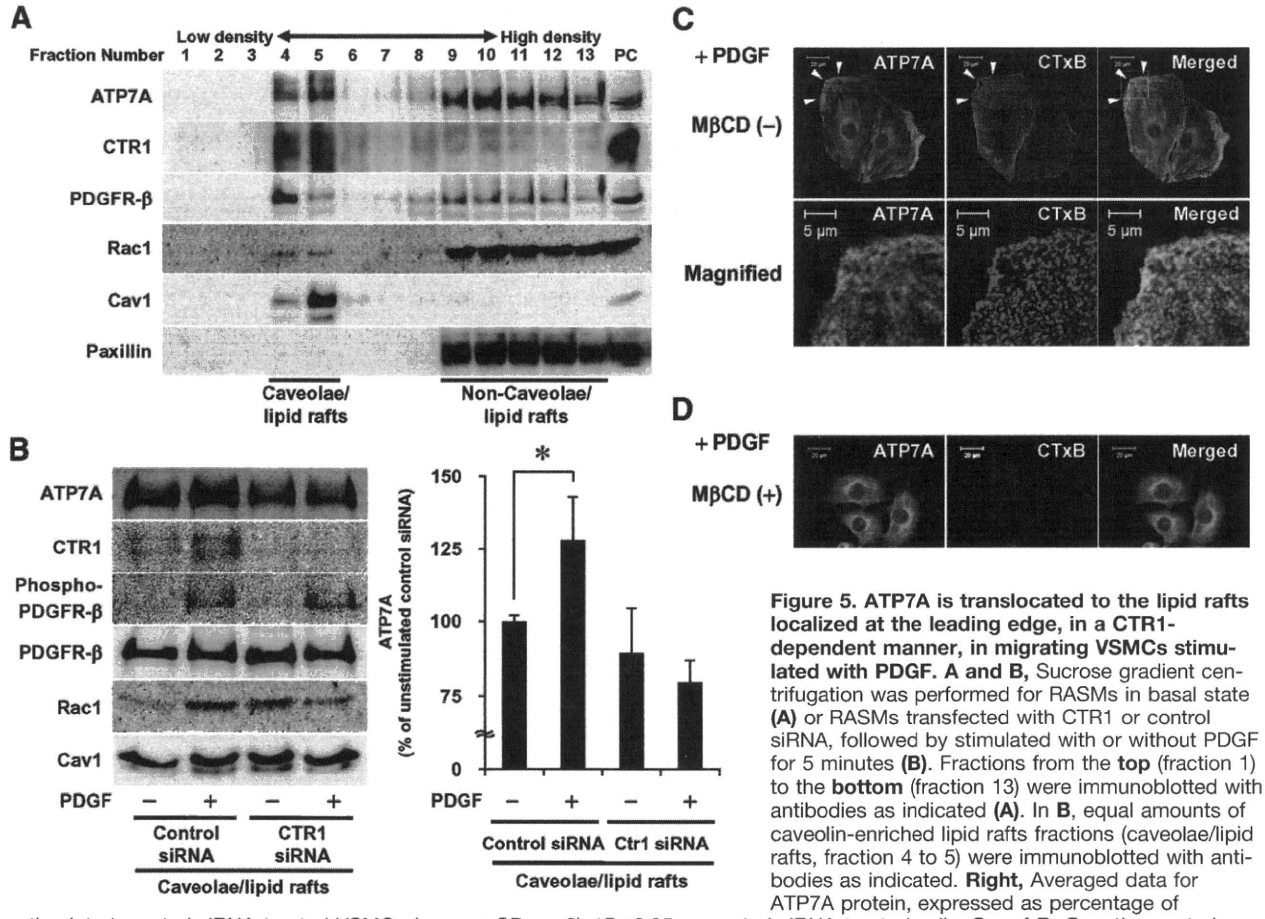

Figure 5. ATP7A is translocated to the lipid rafts localized at the leading edge, in a CTR1-dependent manner, in migrating VSMCs stimulated with PDGF. A and B, Sucrose gradient centrifugation was performed for RASMs in basal state **(A)** or RASMs transfected with CTR1 or control siRNA, followed by stimulated with or without PDGF for 5 minutes **(B)**. Fractions from the **top** (fraction 1) to the **bottom** (fraction 13) were immunoblotted with antibodies as indicated **(A)**. In **B**, equal amounts of caveolin-enriched lipid rafts fractions (caveolae/lipid rafts, fraction 4 to 5) were immunoblotted with antibodies as indicated. **Right,** Averaged data for ATP7A protein, expressed as percentage of unstimulated, control siRNA-treated VSMCs (means±SD, n=3). *$P<0.05$ vs control siRNA-treated cells. **C and D,** Growth-arrested RASMs were treated with **(C)** or without **(D)** 10 mmol/L methyl-β-cyclodextrin for 2 hours and stimulated with 50 ng/mL PDGF for 5 minutes. Cells were costained with anti-ATP7A antibody **(green)** and Alexa 555–CTxB **(red)**. All fluorescence images were taken at 5 different fields/well and are representative of >3 different experiments.

efflux and ^{64}Cu uptake experiments in cultured VSMCs and found that PDGF stimulation had no effects on either response (Online Figure VII). Similarly, ICP-MS analysis of total cell lysates of VSMCs also showed that copper contents were not changed after PDGF stimulation (Figure 6A). Because ATP7A is recruited to the caveolae/lipid rafts in response to PDGF, we next measured the copper content in the lipid rafts and nonlipid raft fractions. Intriguingly, we found that the caveolae/lipid rafts fraction contains much higher amounts of copper than nonlipid raft fractions in the basal state (Figure 6B). Moreover, PDGF stimulation significantly reduced copper content in caveolae/lipid rafts in an ATP7A-dependent manner (Figure 6C and Online Figure VIII). These results suggest that PDGF-induced recruitment of ATP7A to the lipid rafts may contribute to copper export to the extracellular space in these specialized microdomains. This was not detected by global measurements of ^{64}Cu efflux and ^{64}Cu uptake in whole cells. The plasma membrane localization of ATP7A and CTR1 in PDGF-stimulated VSMCs was confirmed by using cell surface biotinylation assays (Online Figure IX).

We next examined whether PDGF-induced decrease in copper content in caveolae/lipid rafts may reflect the secretion of copper-binding proteins, such as Pro-LOX which obtain copper from ATP7A. We found that pro-LOX was localized in caveolae/lipid rafts in the basal state, and PDGF stimulation promoted the reduction of pro-LOX level in an ATP7A dependent manner in these fractions (Figure 6D and 6E; Online Figure X). After secretion, Pro-LOX is processed to a mature active nonglycosylated LOX and a glycosylated propeptide LOX-PP.[22,23] Of note, LOX and LOX-PP were not found in caveolae/lipid rafts in the basal state or after PDGF treatment (Figure 6D and 6E). Taken together, these findings suggest that PDGF-stimulated ATP7A recruitment into the caveolae/lipid rafts may be required for the secretion of copper-dependent enzymes such as pro-LOX localized in these specific compartments.

It has been reported that ATP7A is involved in LOX activity[17,36] and that LOX activity is involved in PDGF-induced VSMC migration[24] in addition to its effect on extracellular matrix remodeling. We thus examined whether LOX activity is involved in copper transporter ATP7A-dependent PDGF-induced VSMC migration. ATP7AsiRNA significantly inhibited LOX activity in VSMCs treated with PDGF (Online Figure XII, A). Furthermore, treatment of a specific chemical LOX activity inhibitor, βaminopropion-

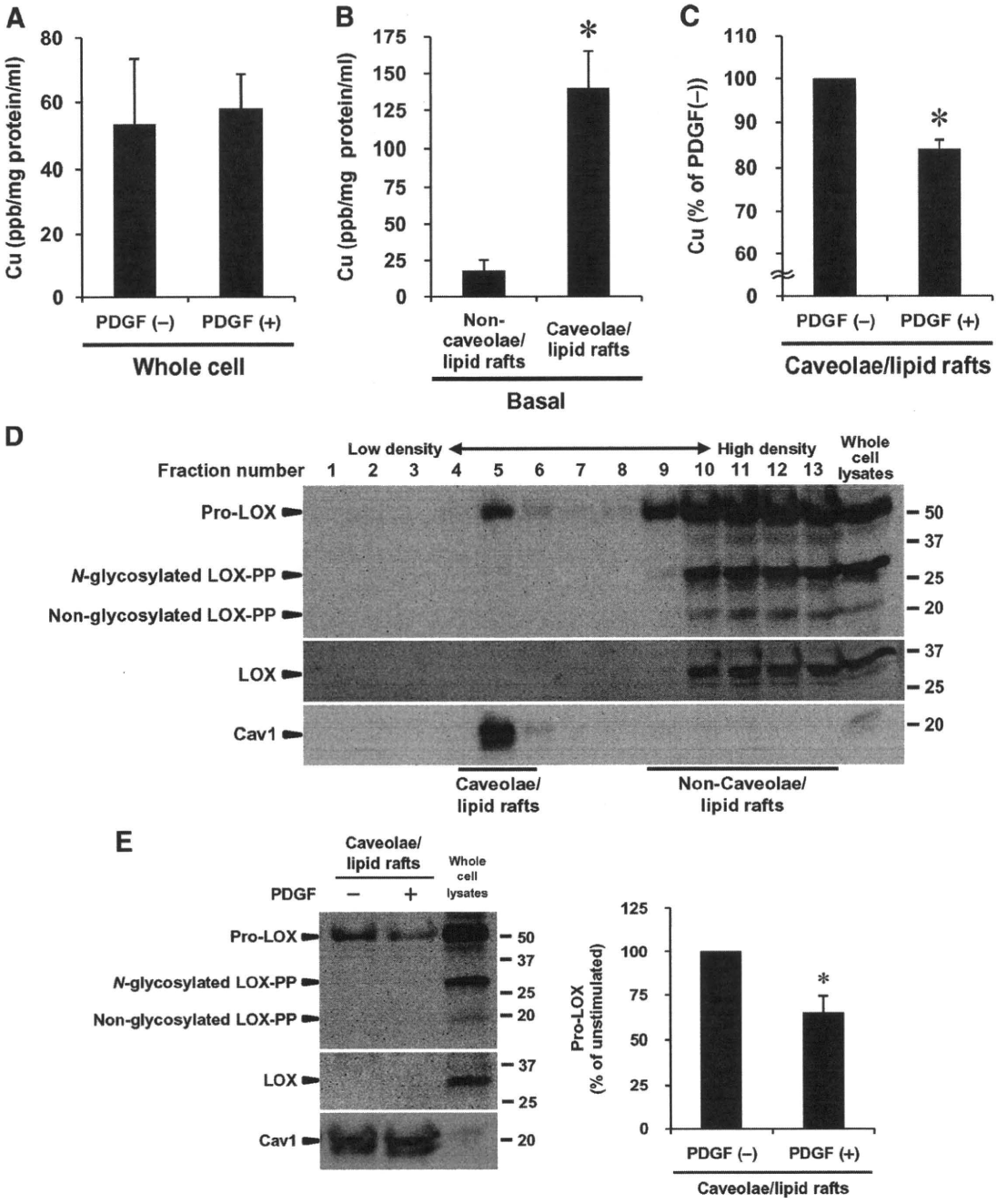

Figure 6. PDGF stimulation reduces copper content and Pro-LOX in lipid rafts fractions in VSMCs. A through C, Copper contents were measured by ICP-MS in whole cells **(A)** or caveolae/lipid rafts or noncaveolae/lipid rafts **(B and C)** in RASMs with or without PDGF stimulation for 5 minutes. Equal amounts of proteins in caveolae/lipid rafts (fractions 4 to 5) or noncaveolae/lipid rafts (fractions 9 to 13) were obtained by sucrose gradient fractionation as described for Figure 5. *$P<0.05$ vs nonlipid rafts or unstimulated cells (means±SD, n=3). **D,** Identification of Pro-LOX, but not LOX, in caveolae/lipid rafts in VSMCs. RASMs were fractionated by sucrose gradient centrifugation, followed by immunoblotted with anti–LOX-PP (which detects both Pro-Lox and LOX-PP), anti-LOX, or anti–caveolin-1 antibodies. **E,** Effect of PDGF treatment on Pro-LOX level in caveolae/lipid rafts fractions in VSMCs. Equal amounts of proteins in caveolae/lipid rafts (fractions 4 to 5) were immunoblotted with anti–LOX-PP, -LOX, or –caveolin-1 antibodies in RASMs with or without 50 ng/mL PDGF for 5 minutes.

itrile (BAPN), significantly inhibits PDGF-induced VSMC migration (Online Figure XII, B), which is consistent with the report by Lucero et al.[24] These findings suggest that LOX activity is involved in PDGF-induced, ATP7A-dependent VSMC migration.

ATP7A Is Upregulated in Neointimal Formation in Response to Vascular Injury In Vivo

To determine the functional significance of ATP7A in VSMC migration in vivo, we examined the role of ATP7A in neointimal formation using a mouse wire injury model.

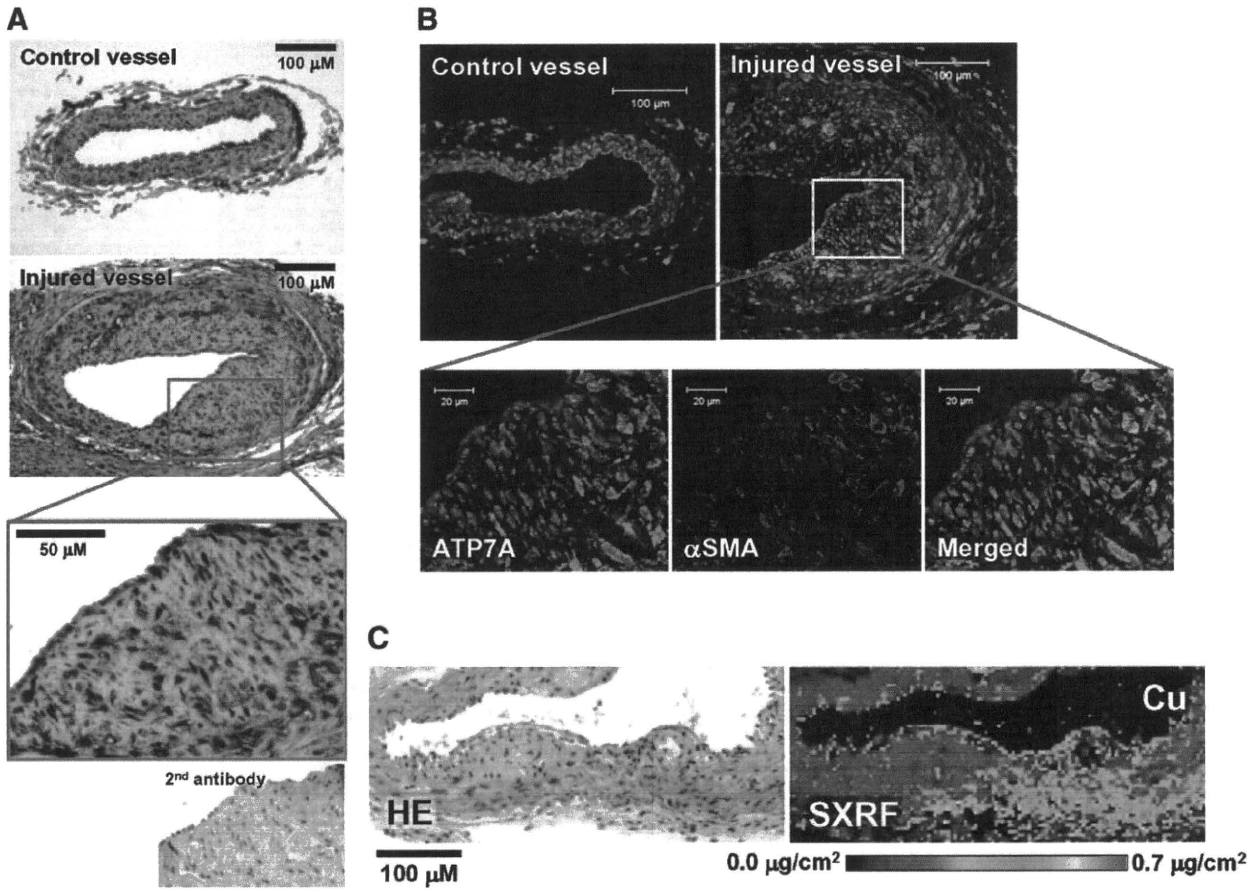

Figure 7. ATP7A is involved in neointimal formation in response to vascular injury in vivo. A and B, ATP7A is highly expressed in neointimal VSMCs of wire-injured carotid arteries of ApoE-deficient atherosclerotic mice. Immunohistochemical **(A)** or immunofluorescence **(B)** analysis for uninjured (control) or injured (4 weeks after) carotid artery stained with anti-ATP7A antibody **(A)**; or costained with anti- ATP7A **(green)** and α-smooth muscle actin **(red)** antibodies **(B)**. **C,** X-ray fluorescence microscopy scans of the neointima of wire-injured carotid arteries. Areas of neointimal lesions were identified by hematoxylin/eosin staining **(left)**. X-ray fluorescence microscopy scans (1 to 2 seconds per pixel) were performed in paraffin-embedded tissue **(right)**. Map of Cu shows areas of the lowest to the highest content scaled to a rainbow color **(bottom)**. Copper accumulation in neointimal lesions is shown in **white arrow**. The minimal and maximal Cu content displayed in micrograms per square centimeter is shown in the image.

Immunohistochemical analysis showed that ATP7A protein expression was robustly increased in neointimal VSMC and endothelial cells lining the lumen in the injured vessel of ApoE-deficient atherosclerotic mice (Figure 7A). Immunofluorescence analysis demonstrated that ATP7A was colocalized with α-smooth muscle actin, a VSMC marker, in the neointima formed in response to injury (Figure 7B). We next examined if induction of ATP7A precedes VSMC migration after injury to address the cause-effect of ATP7A in VSMC migration in vivo. As shown in Online Figure XI, we observed increase in ATP7A expression at 3 days after wire injury in the vessels of ApoE-deficient atherosclerotic mice, whereas there was no VSMC migration and neointima formation at this time point as reported by Linder et al.[37] Thus, these findings suggest that ATP7A expression is increased before the onset of VSMC migration following vascular injury and this upregulation is also observed in neointimal VSMCs. Finally, we examined spatial distribution of copper in neointima using synchrotron-based x-ray fluorescence microscopy (SXFM).[28] As shown in Figure 7C, copper accumulation was observed at neointimal lesions in wire injury model. These results suggest that ATP7A may be involved in neointima formation in response to vascular injury in vivo.

Discussion

A role for copper in tissue repair, neointima thickening and atherosclerosis has been suggested; however, the underlying detailed mechanisms remain unknown.[3–7,9–11] Here we provide novel evidence that the ATP7A copper transporter is involved in PDGF-stimulated VSMC migration, which is critical for neointimal formation and vascular remodeling (Figure 8). We found that stimulation with PDGF promotes ATP7A translocation from TGN to the leading edge. This PDGF-induced ATP7A movement toward the site of actin remodeling is inhibited by cell permeable and impermeable copper chelators as well as depletion of the CTR1 copper importer. It has been shown that relocalization of ATP7A from the Golgi is triggered by increased cytoplasmic copper as well as by estrogen, insulin, NMDA (*N*-methyl-D-aspartate) activation, hypoxia, and cytokines.[2,16,38,39] However, our data are the first demonstration that the ATP7A